ADVANCED THEORY AND SIMULATIONS
www.advtheorysimul.com

Mathematical Exploration of Malaria Transmission Dynamics: Insights from Fractional Models and Numerical Simulation

Souad Bounouiga, Bilal Basti, and Noureddine Benhamidouche*

This study presents an innovative mathematical model denoted as the fractional SIP(H)–SI(M) model, which aims to analyze and understand the dynamics of malaria transmission and spread. This model is distinguished by incorporating memory effects through fractional differential equations, allowing for a more accurate and realistic analysis of disease spread compared to traditional models. The proposed model is applied to Algeria by estimating its parameters using recent health data (from 2000). The results revealed that the disease-free equilibrium is stable only when the basic reproduction number is less than one, indicating that controlling the spread of malaria and possibly eradicating it can be achieved by implementing appropriate preventive measures. Simulations also demonstrated a direct correlation between the rate of infection transmission and an increase in the number of infected individuals, highlighting the need for swift action when signs of an outbreak emerge. Based on these findings, a set of preventive measures is recommended, including insecticide spraying programs, widespread distribution of insecticide-treated bed nets, and implementation of effective treatment protocols for infected individuals. This study also emphasizes the importance of continuous monitoring of health data and updating model parameters to ensure the effectiveness and sustainability of preventive measures.

1. Introduction

The transmission of diseases through mosquito bites highlights the important role of small pests in the spread of diseases. Malaria, which results from blood parasites of the genus Plasmodium and is transmitted through Anopheles mosquito bites, poses a major challenge to human health. This disease is notorious for its prevalence in tropical and subtropical regions, where the environment is conducive to mosquito breeding and transmission of blood parasites between humans. Global Health Organizations estimate that the number of malaria cases annually ranges from hundreds of thousands to millions, with developing countries being particularly affected.

Suitable environmental conditions such as stagnant water pools and high temperatures contribute to the spread of malaria, increase its severity, and exacerbate its complications. Those afflicted with malaria suffer from serious health effects, including organ failure such as kidney and liver failure, changes in blood composition, and central nervous system disorders. Individuals infected with malaria may experience symptoms such as high fever, severe headache, muscle pain, and confusion. In severe cases, death may occur if immediate and adequate treatment are not administered. Therefore, combating mosquitoes is of paramount importance for reducing the transmission of this disease and preserving public health.

With advances in technology and mathematics, mathematical modeling has become a powerful tool for understanding and analyzing the dynamics of disease spread.[1–7] Recent studies have increasingly highlighted the importance of incorporating memory and hereditary characteristics into disease models through fractional calculus. Traditional models rely on integer-order derivatives, which may be insufficient for representing complex dynamic phenomena involving memory effects. In contrast, fractional derivatives allow for a more accurate representation of these processes by considering not only the current state of the system but also the entire history of previous states. This approach provides a more comprehensive framework for analyzing disease dynamics, enabling the modeling of time-dependent factors such as acquired immunity, recurrent infections, and environmental changes that influence disease transmission.

The superiority of fractional models over traditional integer-order models lies in their ability to represent memory effects and long-term dependencies, which are crucial for understanding and controlling the spread of infectious diseases such as malaria. For example, recent research has shown that fractional differential equations can more accurately model disease spread in populations with varying susceptibility and exposure, leading to better predictions and more effective intervention strategies refs. [8–17]. In addition, fractional models allow for a more

S. Bounouiga, B. Basti, N. Benhamidouche
Laboratory of Pure and Applied Mathematics
Mohamed Boudiaf University of M'sila
M'sila 28000, Algeria
E-mail: bilal.basti@univ-msila.dz

The ORCID identification number(s) for the author(s) of this article can be found under https://doi.org/10.1002/adts.202400630

DOI: 10.1002/adts.202400630

precise representation of time-dependent processes such as seasonal variations or the impact of health interventions, which may have long-lasting effects. This precision in representation makes fractional models an essential tool for designing disease-control strategies that account for the real complexities of ecological and health systems.

In addition to their application in disease modeling, fractional differential equations have been used in various fields, including optimization problems, medical diagnosis, and artificial intelligence, offering a more comprehensive framework for analyzing complex systems.[18–24] As this field continues to evolve, the integration of these advanced mathematical tools is expected to play a crucial role in shaping future public health policies and interventions, not only in combating malaria but also in addressing numerous other global health challenges.

This study contributes to the development of a fractional mathematical model aimed at enhancing our understanding of the malaria transmission dynamics. The effectiveness of the model in accurately representing disease dynamics is ensured by analyzing the equilibrium points and studying the solution stability. Additionally, calculating the basic reproduction number provides crucial insights into the disease spread rate and influencing factors, which aids in better guiding health policies and preventive measures. Moreover, the model is used to validate the data and identify the factors contributing to disease transmission. Based on the results of the model, recommendations and strategies are offered to improve malaria control efforts and reduce their impact on public health.

In our study concerning the dynamics of the epidemic, we categorize the entire human population, represented as H, into three distinct classes: Susceptible (S_H), Infected (I_H), and Partially Immune (P_H) individuals.

Moreover, the mosquito population surrounding the human population, denoted as M, is partitioned into two distinct categories: Susceptible (S_M) and Infected (I_M) mosquitoes.

The parameters of the SIP(H)–SI(M) model are defined as follows:

1) Λ indicates the rate of increase in the susceptible individuals.
2) λ represents the rate of increase in the susceptible mosquitoes.
3) $\mu < \Lambda$ is the rate of natural death for humans.
4) $\upsilon < \lambda$ represents the rate of natural death of mosquitoes.
5) β is the probability rate of disease transmission from I_M to S_H.
6) γ is the probability rate of disease transmission from I_H to S_M.
7) κ expresses the immunity acquisition rate for humans.
8) δ represents the immunity loss rate for humans.

Fractional calculus has become increasingly essential and is considered a possible alternative to integer-order models. This allows for the description and processing of a wide range of structural properties within the studied system. Caputo's definitions allow the initial conditions to be expressed significantly as traditional derivatives, making them the preferred fractional derivatives for many mathematical modeling applications. Interested readers can delve deeper into this topic by referring to refs. [18, 23, 25–34].

Motivated by the above-mentioned work, for $0 \le t \le \ell < \infty$, and $0 < \alpha \le 1$, we have:

$$\begin{cases} {}^{C}D^{\alpha}_{0^+} S_H(t) = \Lambda H(t) + \delta P_H(t) - \left(\dfrac{\beta I_M(t)}{M(t)} + \mu\right) S_H(t) \\ {}^{C}D^{\alpha}_{0^+} I_H(t) = \dfrac{\beta I_M(t)}{M(t)} S_H(t) - (\kappa + \mu) I_H(t) \\ {}^{C}D^{\alpha}_{0^+} P_H(t) = \kappa I_H(t) - (\delta + \mu) P_H(t) \\ {}^{C}D^{\alpha}_{0^+} S_M(t) = \lambda M(t) - \left(\dfrac{\gamma I_H(t)}{H(t)} + \upsilon\right) S_M(t) \\ {}^{C}D^{\alpha}_{0^+} I_M(t) = \dfrac{\gamma I_H(t)}{H(t)} S_M(t) - \upsilon I_M(t) \end{cases} \tag{1}$$

where the first three equations in system (1) represent human equations, while the last two equations express mosquito equations.

The changes in the transmission of infectious diseases between humans and mosquitoes in SIP(H)–SI(M) model (1) can be interpreted as follows:

In **Figure 1**, it is assumed that susceptible individuals S_H are recruited at a rate ΛH and die naturally at a rate μ. They become infected with malaria as a result of being bitten by infected mosquitoes and moving to infected class I_H at a transmission rate β.

For infected individuals, I_H is assumed to die naturally at a rate μ or acquire partial temporary immunity and move to the partially immune class P_H at a rate κ. Furthermore, partially immune individuals' P_H may lose immunity and return to the susceptible class S_H at a rate δ or die naturally at a rate μ.

As for mosquitoes S_M, they are recruited into the susceptible category at a rate λM and die naturally at a rate υ. Susceptible mosquitoes S_M become infected with malaria at a rate γ after feeding on the blood of infected humans and move to the infected humans and move to the infected category I_M. Infected mosquitoes I_M also die naturally at a rate υ.

The paper is structured to gain a thorough understanding of malaria transmission dynamics and the factors that influence them. We begin with exploring the feasibility region for the fractional SIP(H)–SI(M) mathematical model using the Caputo fractional derivative. This allows us define the boundaries in which we can effectively analyze the system's behavior and disease spread. This analysis helps in assessing the model's applicability and identifying the optimal conditions for its study.

Following this, attention is focused on studying the existence, uniqueness, and stability of solutions using Schauder's and Banach's fixed-point theorems, along with Ulam–Hyers' stability criteria. This analysis ensures that the model provides sustainable and applicable solutions, enhancing its credibility and ability to accurately represent real-world dynamics.

The basic reproduction number, $\mathfrak{R}_0$, is a critical indicator for assessing malaria transmission. Determining $\mathfrak{R}_0$ provides insights into disease spread rates and helps to identify points where control measures can be applied. In addition, we investigate the equilibrium points within the fractional SIP(H)–SI(M) model, analyze their stability to guide disease control strategies, and predict future trends. Mosquitoes play a crucial role in the transition between susceptible and infected states. Their recruitment,

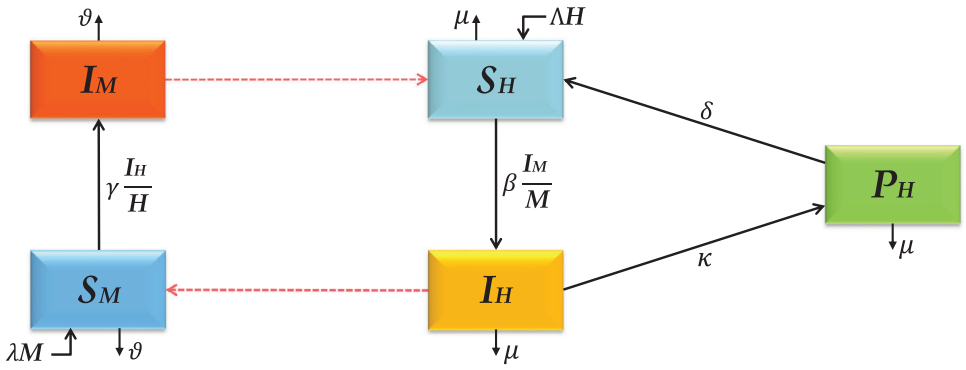

Figure 1. Flowchart of SIP(H)–SI(M).

natural mortality, and infection dynamics are integral components of our model.

We validate the accuracy of our model using real data from the Algerian region. This allows us to identify the specific local factors contributing to the spread of malaria. The validation process enhances the precision of the model and assists in developing targeted disease-control strategies. Furthermore, we investigate the memory effect, which has enriched our understanding of the influence of temporal and historical dynamics on disease transmission.

2. Necessary Definitions and Preliminaries

This section aims to clarify some fundamental definitions that result from the fractional calculus theory. The space under consideration is the Banach space of continuous functions $C([0,\ell],\mathbb{C})$, with the norm

$$\|\varphi\|_\infty = \sup_{t\in[0,\ell]} |\varphi(t)| \tag{2}$$

Definition 1 (Ref. [22]). *The left-sided (arbitrary) fractional integral of order $\alpha > 0$ of a continuous function $\varphi : [0,\ell] \to \mathbb{R}$ is given by*

$$\mathcal{J}^{\alpha}_{0^+}\varphi(t) = \frac{1}{\Gamma(\alpha)}\int_0^t (t-\tau)^{\alpha-1}\varphi(\tau)d\tau,\ t\in[0,\ell] \tag{3}$$

where $\Gamma(\alpha) = \int_0^\infty \tau^{\alpha-1}\exp(-\tau)\,d\tau$ is the Euler gamma function.

Definition 2 (Caputo's fractional derivative [22]). *The left-sided Caputo's fractional derivative of order $\alpha > 0$ of a function $\varphi : [0,\ell] \to \mathbb{R}$ is given by*

$${}^{C}\mathcal{D}^{\alpha}_{0^+}\varphi(t) = \begin{cases} \dfrac{d^m\varphi(t)}{dt^m},\ \text{for } \alpha = m \in \mathbb{N}_0, \\ \mathcal{J}^{m-\alpha}_{0^+}\dfrac{d^m\varphi(t)}{dt^m} = \displaystyle\int_0^t \frac{(t-\tau)^{m-\alpha-1}}{\Gamma(m-\alpha)}\frac{d^m\varphi(\tau)}{d\tau^m}d\tau, \\ \qquad\qquad \text{for } m-1 < \alpha < m \in \mathbb{N} \end{cases} \tag{4}$$

Lemma 3 (Ref. [22]). *Assume that ${}^{C}\mathcal{D}^{\alpha}_{0^+}\varphi \in C([0,\ell],\mathbb{R})$, then we get for all $\alpha > 0$*

$$\mathcal{J}^{\alpha}_{0^+}\,{}^{C}\mathcal{D}^{\alpha}_{0^+}\varphi(t) = \varphi(t) - \sum_{k=0}^{n-1}\frac{\varphi^{(k)}(0)}{k!}t^k,\ n-1 < \alpha \le n \in \mathbb{N} \tag{5}$$

Lemma 4 (Gronwall [19]). *Let $\varphi(t)$ and $\omega(t)$ be nonnegative, continuous functions on $0 \le t \le \ell$, for which the inequality:*

$$\varphi(t) \le \varphi(0) + \int_0^t \omega(\tau)\varphi(\tau)d\tau,\ t\in[0,\ell] \tag{6}$$

where $\varphi(0)$ is a nonnegative constant. Then

$$\varphi(\tau) \le \varphi(0)\exp\left(\int_0^t \omega(\tau)d\tau\right),\ t\in[0,\ell] \tag{7}$$

3. Dynamic Analysis of the Feasible Region

3.1. Positivity and Boundedness of the Model

The SIP(H)–SI(M) model (1) is investigated within a biologically feasible region in $\mathbb{R}^5_+$, as defined in the subsequent lemma.

Lemma 5. *Assume that M_0 repersents the initial total mosquito population, let H_0 be the initial total human population at $t = 0$, where $0 \le t \le \ell \le \infty$. Consequently, the solution to the considered model is confined to the feasible region, given by*

$$\Omega = \left\{ (S_H, I_H, P_H, S_M, I_M) \in \mathbb{R}^5_+ : 0 \le H(t) \le H_0\exp\left(\frac{\Lambda\ell^\alpha}{\Gamma(\alpha+1)}\right),\right.$$
$$\left. 0 \le M(t) \le M_0\exp\left(\frac{\lambda\ell^\alpha}{\Gamma(\alpha+1)}\right)\right\}. \tag{8}$$

with

$$H(t) = S_H(t) + I_H(t) + P_H(t), \qquad M(t) = S_M(t) + I_M(t) \tag{9}$$

Proof. Let

$$H(t) = S_H(t) + I_H(t) + P_H(t) \tag{10}$$

then

$$ {}^{C}\mathcal{D}^{\alpha}_{0^+} H(t) = {}^{C}\mathcal{D}^{\alpha}_{0^+} S_H(t) + {}^{C}\mathcal{D}^{\alpha}_{0^+} I_H(t) + {}^{C}\mathcal{D}^{\alpha}_{0^+} P_H(t) \tag{11} $$

Now, summing all the human equations of (1), we get

$$ \begin{aligned} {}^{C}\mathcal{D}^{\alpha}_{0^+} H(t) &= (\Lambda - \mu) H(t) \\ &\leq \Lambda H(t) \end{aligned} \tag{12} $$

After using Lemma 3, we get

$$ H(t) \leq H_0 + \Lambda \mathcal{J}^{\alpha}_{0^+} H(t) \tag{13} $$

Applying Gronwall Lemma 4, we obtain

$$ H(t) \leq H_0 \exp\left(\frac{\Lambda \ell^{\alpha}}{\Gamma(\alpha+1)} \right) \tag{14} $$

where H_0 is the total human population at $t = 0$.

In another way, let

$$ M(t) = S_M(t) + I_M(t) \tag{15} $$

then

$$ {}^{C}\mathcal{D}^{\alpha}_{0^+} M(t) = {}^{C}\mathcal{D}^{\alpha}_{0^+} S_M(t) + {}^{C}\mathcal{D}^{\alpha}_{0^+} I_M(t) \tag{16} $$

Now, summing all the mosquito equations of (1), we obtain

$$ \begin{aligned} {}^{C}\mathcal{D}^{\alpha}_{0^+} M(t) &= (\lambda - \upsilon) M(t) \\ &\leq \lambda M(t) \end{aligned} \tag{17} $$

Applying Lemma 3, gives us

$$ M(t) \leq M_0 + \lambda \mathcal{J}^{\alpha}_{0^+} M(t) \tag{18} $$

After using Gronwall Lemma 4, we get

$$ M(t) \leq M_0 \exp\left(\frac{\lambda \ell^{\alpha}}{\Gamma(\alpha+1)} \right) \tag{19} $$

where M_0 is the total mosquito population at $t = 0$.

In subsequent sections of this paper, we assume the existence of two positive constants:

$$ \mathcal{H} \leq H_0 \exp\left(\tfrac{\Lambda \ell^{\alpha}}{\Gamma(\alpha+1)} \right), \qquad \mathcal{M} \leq M_0 \exp\left(\tfrac{\lambda \ell^{\alpha}}{\Gamma(\alpha+1)} \right) \tag{20} $$

where the total human population H and mosquito population M remained fixed throughout the study period and can be expressed as $H(t) = \mathcal{H}$ and $M(t) = \mathcal{M}$. This assumption was made to normalize the SIP(H)–SI(M) model (1). Therefore, we put:

$$ \begin{aligned} S(t) &= \frac{S_H(t)}{\mathcal{H}}, \qquad I(t) = \frac{I_H(t)}{\mathcal{H}}, \qquad P(t) = \frac{P_H(t)}{\mathcal{H}} \\ V(t) &= \frac{S_M(t)}{\mathcal{M}}, \qquad F(t) = \frac{I_M(t)}{\mathcal{M}}, \end{aligned} \tag{21} $$

then we obtain

$$ \begin{cases} {}^{C}\mathcal{D}^{\alpha}_{0^+} S(t) = \Lambda + \delta P(t) - (\beta F(t) + \mu) S(t) \\ {}^{C}\mathcal{D}^{\alpha}_{0^+} I(t) = \beta F(t) S(t) - (\kappa + \mu) I(t) \\ {}^{C}\mathcal{D}^{\alpha}_{0^+} P(t) = \kappa I(t) - (\delta + \mu) P(t) \\ {}^{C}\mathcal{D}^{\alpha}_{0^+} V(t) = \lambda - (\gamma I(t) + \upsilon) V(t) \\ {}^{C}\mathcal{D}^{\alpha}_{0^+} F(t) = \gamma I(t) V(t) - \upsilon F(t) \end{cases} \tag{22} $$

along with the positive initial conditions

$$ S(0) = \varphi_1, \; I(0) = \varphi_2, \; P(0) = \varphi_3, \; V(0) = \varphi_4, \; F(0) = \varphi_5 \tag{23} $$

3.2. Existence Results of Solutions for the Normalized Model

In this section, we explore the existence and uniqueness of solutions to problem in Equations (26)–(27) through the field of fixed-point theory. Our investigation employs Banach's and Schauder's fixed-point theorems, as outlined in refs. [19, 35–39].

Let $\varphi = (S, I, P, V, F) \in \Omega$, where $\Omega = [C([0, \ell], [0, 1])]^5$ is a Banach space with

$$ \|\varphi\|_{\Omega} = \max\left\{ \|S\|_{\infty}, \|I\|_{\infty}, \|P\|_{\infty}, \|V\|_{\infty}, \|F\|_{\infty} \right\} \tag{24} $$

and let $\psi = (\psi_1, \psi_2, \psi_3, \psi_4, \psi_5)$, be such that

$$ \begin{cases} \psi_1(t, \varphi(t)) = \Lambda - (\beta F(t) + \mu) S(t) + \delta P(t) \\ \psi_2(t, \varphi(t)) = \beta F(t) S(t) - (\kappa + \mu) I(t) \\ \psi_3(t, \varphi(t)) = \kappa I(t) - (\delta + \mu) P(t) \\ \psi_4(t, \varphi(t)) = \lambda - (\gamma I(t) + \upsilon) V(t) \\ \psi_5(t, \varphi(t)) = \gamma I(t) V(t) - \upsilon F(t) \end{cases} \tag{25} $$

It is clear that ψ is a continuous function.

By applying $\mathcal{J}^{\alpha}_{0^+}$ to both sides of the system

$$ {}^{C}\mathcal{D}^{\alpha}_{0^+} \varphi(t) = \psi(t, \varphi(t)) \tag{26} $$

taking into account the conditions

$$ \varphi(0) = \varphi_0 = (\varphi_1, \varphi_2, \varphi_3, \varphi_4, \varphi_5) \tag{27} $$

and employing Lemma 3, we obtain the following system of fractional integral equations

$$ \varphi(t) = \varphi_0 + \frac{1}{\Gamma(\alpha)} \int_0^t (t - \tau)^{\alpha - 1} f(\tau, \varphi(\tau)) d\tau \tag{28} $$

which is equivalent to the original problem in Equations (26)–(27).

Theorem 6. *Let $\beta, \gamma, \delta, \kappa, \upsilon, \mu, \alpha, \ell \in \mathbb{R}_+$, be such that $\alpha \in (0, 1]$ and*

$$ \ell < \left(\frac{\Gamma(\alpha + 1)}{\max\{\beta + \mu, \kappa + \mu, \delta + \mu, \gamma + \upsilon\}} \right)^{\frac{1}{\alpha}} \tag{29} $$

Then, there is at least one solution to problem in Equations (26)–(27) on $[0, \ell]$.

Proof. The proof begins with transformation of problem in Equations (26)–(27) into a fixed-point problem $\mathcal{T}\varphi(t) = \varphi(t)$, with

$$\mathcal{T}\varphi(t) = \left(\mathcal{T}_1\varphi(t), \mathcal{T}_2\varphi(t), \mathcal{T}_3\varphi(t), \mathcal{T}_4\varphi(t), \mathcal{T}_5\varphi(t)\right) \tag{30}$$

and

$$\mathcal{T}\varphi(t) = \varphi_0 + \frac{1}{\Gamma(\alpha)}\int_0^t (t-\tau)^{\alpha-1}\psi(\tau, \varphi(\tau))d\tau \tag{31}$$

Observing that for $\varphi \in \Omega$, the operators $\mathcal{T}_i\varphi$ for $1 \le i \le 5$ are continuous, as demonstrated in Step 1. Consequently, $\mathcal{T}\varphi$ is an element of Ω, with

$$\|\mathcal{T}\varphi\|_\Omega = \max_{1\le i\le 5}\left\|\mathcal{T}_i\varphi\right\|_\infty \tag{32}$$

The equivalence between problems in Equations (26)–(27) and (31) implies that $\mathcal{T}$ includes fixed points for solving the aforementioned problem.

Step 1. $\mathcal{T}$ is a continuous operator. Let $\left(\varphi_n\right)_{n\in\mathbb{N}_0} = \left(S_n, I_n, P_n, V_n, F_n\right)$ be five nonnegative real sequences, such that $\lim_{n\to\infty}\varphi_n = \varphi$ in Ω. We obtain for all $t \in [0, \ell]$,

$$\begin{aligned}&\left|\mathcal{T}_i\varphi_n(t) - \mathcal{T}_i\varphi(t)\right| \\ &\le \frac{1}{\Gamma(\alpha)}\int_0^t (t-\tau)^{\alpha-1}\left|\psi_i\left(\tau, \varphi_n(\tau)\right) - \psi_i(\tau, \varphi(\tau))\right|d\tau\end{aligned} \tag{33}$$

where ψ_i satisfies in Equation(25) for each $1 \le i \le 5$. We have

$$\begin{aligned}\left|\psi_1\left(t, \varphi_n(t)\right) - \psi_1(t, \varphi(t))\right| &= \left|\delta\left(P_n(t) - P(t)\right) - \left[\left(\beta F_n(t) + \mu\right)S_n(t)\right.\right. \\ &\quad \left.\left. - \left(\beta F(t) + \mu\right)S(t)\right]\right| \\ &\le \delta\left|P_n(t) - P(t)\right| + \mu\left|S_n(t) - S(t)\right| \\ &\quad + \left|\beta F_n(t)S_n(t) - \beta F(t)S(t)\right| \\ &\le \delta\left|P_n(t) - P(t)\right| + (\beta + \mu)\left|S_n(t) - S(t)\right| \\ &\quad + \beta\left|F_n(t) - F(t)\right| \\ &\le \max\{\delta, \beta + \mu\}\left\|\varphi_n - \varphi\right\|_\Omega\end{aligned} \tag{34}$$

Similarly, we obtain

$$\begin{aligned}\left|\psi_2\left(t, \varphi_n(t)\right) - \psi_2(t, \varphi(t))\right| &\le \max\{\beta, \kappa + \mu\}\left\|\varphi_n - \varphi\right\|_\Omega \\ \left|\psi_3\left(t, \varphi_n(t)\right) - \psi_3(t, \varphi(t))\right| &\le \max\{\kappa, \delta + \mu\}\left\|\varphi_n - \varphi\right\|_\Omega \\ \left|\psi_4\left(t, \varphi_n(t)\right) - \psi_4(t, \varphi(t))\right| &\le (\gamma + \upsilon)\left\|\varphi_n - \varphi\right\|_\Omega \\ \left|\psi_5\left(t, \varphi_n(t)\right) - \psi_5(t, \varphi(t))\right| &\le \max\{\gamma, \upsilon\}\left\|\varphi_n - \varphi\right\|_\Omega\end{aligned} \tag{35}$$

Since $\varphi_n \to \varphi$ in Ω as $n \to \infty$, we get $\psi_i\left(t, \varphi_n(t)\right) \to \psi_i(t, \varphi(t))$ for any $t \in [0, \ell]$, and each $i \in \overline{1,5}$.

Now, let $\mathcal{K} > 0$, be such that for each $t \in [0, \ell]$, we have

$$\begin{aligned}&\frac{(t-\tau)^{\alpha-1}}{\Gamma(\alpha)}\left|\psi_i\left(\tau, \varphi_n(\tau)\right) - \psi_i(\tau, \varphi(\tau))\right| \\ &\le \frac{(t-\tau)^{\alpha-1}}{\Gamma(\alpha)}\left(\left|\psi_i\left(\tau, \varphi_n(\tau)\right)\right| + \left|\psi_i(\tau, \varphi(\tau))\right|\right) \\ &\le \frac{2\mathcal{K}}{\Gamma(\alpha)}(t-\tau)^{\alpha-1}\end{aligned} \tag{36}$$

For each $i \in \overline{1,5}$, the function $\tau \to \frac{2\mathcal{K}}{\Gamma(\alpha)}(t-\tau)^{\alpha-1}$ is integrable on $[0, t]$, for each $t \in [0, \ell]$. Thus, the implication of Lebesgue's dominated convergence theorem gives us

$$\left|\mathcal{T}_i\varphi_n(t) - \mathcal{T}_i\varphi(t)\right| \to 0 \text{ as } n \to \infty \tag{37}$$

and hence

$$\lim_{n\to\infty}\left\|\mathcal{T}\varphi_n - \mathcal{T}\varphi\right\|_\Omega = 0 \tag{38}$$

This signifies the continuity of $\mathcal{T}$.

Step 2. $\mathcal{T}$ is defined from a bounded, closed, and convex subset into itself. Utilizing Equation (29), we define

$$r \ge \frac{\varphi_i\Gamma(\alpha+1) + (\Lambda + \lambda)\ell^\alpha}{\Gamma(\alpha+1) - \max\{\beta + \mu, \kappa + \mu, \delta + \mu, \gamma + \upsilon\}\ell^\alpha} \tag{39}$$

where $\varphi^* = \max_{1\le i\le 5}\varphi_i$, and define the subset Ω_r as follows:

$$\Omega_r = \{\varphi \in \Omega : \|\varphi\|_\Omega \le r\} \tag{40}$$

It is clear that Ω_r is a subset of Ω, distinguished by its bounded, closed, and convex subset of Ω.

Consider the integral operator $\mathcal{T} : \Omega_r \to \Omega$ defined by Equation (31). It follows that $\mathcal{T}\left(\Omega_r\right) \subset \Omega_r$.

Indeed, employing Equations (34) and (35) provides us

$$\begin{aligned}\left|\psi_1(t, \varphi(t))\right| &\le \Lambda + \max\{\beta + \mu, \delta\}\|\varphi\|_\Omega \\ \left|\psi_2(t, \varphi(t))\right| &\le \max\{\beta, \kappa + \mu\}\|\varphi\|_\Omega \\ \left|\psi_3(t, \varphi(t))\right| &\le \max\{\kappa, \delta + \mu\}\|\varphi\|_\Omega \\ \left|\psi_4(t, \varphi(t))\right| &\le \lambda + (\gamma + \upsilon)\|\varphi\|_\Omega \\ \left|\psi_5(t, \varphi(t))\right| &\le \max\{\gamma, \upsilon\}\|\varphi\|_\Omega\end{aligned} \tag{41}$$

Then, in each case, for any $\varphi \in \Omega$

$$\left|\psi_i(t, \varphi(t))\right| \le \eta r, \ \forall i \in \overline{1,5} \tag{42}$$

with

$$\eta = \frac{\Lambda + \lambda}{r} + \max\{\beta + \mu, \kappa + \mu, \delta + \mu, \gamma + \upsilon\} \tag{43}$$

Thus

$$\left|\mathcal{T}_i\varphi(t)\right| \le \varphi_i + \frac{1}{\Gamma(\alpha)}\int_0^t (t-\tau)^{\alpha-1}\left|\psi_i(\tau, \varphi(\tau))\right|d\tau$$

$$\leq \varphi^* + \frac{\eta \ell^\alpha}{\Gamma(\alpha+1)} r$$
$$\leq \varphi^* + \frac{(\Lambda+\lambda)\ell^\alpha}{\Gamma(\alpha+1)} + \frac{\max\{\beta+\mu, \kappa+\mu, \delta+\mu, \gamma+\upsilon\}\ell^\alpha}{\Gamma(\alpha+1)} r$$
$$\leq r, \ \forall i \in \overline{1,5} \tag{44}$$

or $\left(\left\|\mathcal{T}_i\varphi\right\|_\infty\right)_{1\leq i\leq 5} \leq r$, then $\|\mathcal{T}\varphi\|_\Omega \leq r$. Consequently $\mathcal{T}\left(\Omega_r\right) \subset \Omega_r$.

Step 3. $\mathcal{T}\left(\Omega_r\right)$ is equicontinuous subset of Ω.

Let $t_1, t_2 \in [0, \ell]$, $t_1 < t_2$ and $\varphi \in \Omega_r$. Then, for every $i \in \overline{1,5}$, we get

$$\begin{aligned}
&\left|\mathcal{T}_i\varphi(t_2) - \mathcal{T}_i\varphi(t_1)\right| \\
&= \left| \frac{1}{\Gamma(\alpha)} \int_0^{t_2} (t_2-\tau)^{\alpha-1} \psi_i(\tau, \varphi(\tau)) d\tau \right. \\
&\quad \left. - \frac{1}{\Gamma(\alpha)} \int_0^{t_1} (t_1-\tau)^{\alpha-1} \psi_i(\tau, \varphi(\tau)) d\tau \right| \\
&\leq \frac{1}{\Gamma(\alpha)} \int_0^{t_1} \left| \left((t_2-\tau)^{\alpha-1} - (t_1-\tau)^{\alpha-1}\right) \psi_i(\tau, \varphi(\tau)) \right| d\tau \\
&\quad + \frac{1}{\Gamma(\alpha)} \int_{t_1}^{t_2} (t_2-\tau)^{\alpha-1} \left|\psi_i(\tau, \varphi(\tau))\right| d\tau \\
&\leq \frac{\eta r}{\Gamma(\alpha)} \left(\int_0^{t_1} \left| (t_2-\tau)^{\alpha-1} - (t_1-\tau)^{\alpha-1} \right| d\tau \right. \\
&\quad \left. + \int_{t_1}^{t_2} (t_2-\tau)^{\alpha-1} d\tau \right)
\end{aligned} \tag{45}$$

We have

$$(t_2-\tau)^{\alpha-1} - (t_1-\tau)^{\alpha-1} = -\frac{1}{\alpha}\frac{d}{d\tau}\left((t_2-\tau)^\alpha - (t_1-\tau)^\alpha\right) \tag{46}$$

then

$$\int_0^{t_1} \left| (t_2-\tau)^{\alpha-1} - (t_1-\tau)^{\alpha-1} \right| d\tau \leq \frac{1}{\alpha}\left[(t_2-t_1)^\alpha + \left(t_2^\alpha - t_1^\alpha\right)\right] \tag{47}$$

we also have

$$\begin{aligned}
\int_{t_1}^{t_2} (t_2-\tau)^{\alpha-1} d\tau &= -\frac{1}{\alpha}\left[(t_2-\tau)^\alpha\right]_{t_1}^{t_2} \\
&\leq \frac{1}{\alpha}(t_2-t_1)^\alpha
\end{aligned} \tag{48}$$

Then, Equation (45) gives

$$\left|\mathcal{T}_i\varphi(t_2) - \mathcal{T}_i\varphi(t_1)\right| \leq \frac{\eta r}{\Gamma(\alpha+1)}\left[2(t_2-t_1)^\alpha + \left(t_2^\alpha - t_1^\alpha\right)\right] \tag{49}$$

The right-hand side of the inequality above approaches zero as $t_1 \to t_2$ for every $i \in \overline{1,5}$.

Based on Steps 1–3, assisted by the Ascoli–Arzelà theorem, we infer the continuity of $\mathcal{T} : \Omega_r \to \Omega_r$, its compactness, and its satisfaction with Schauder's fixed-point theorem assumptions. Therefore, $\mathcal{T}$ possesses a fixed point that solves problem in Equations (26)–(27) on $[0, \ell]$.

Theorem 7. *We give* $\alpha \in (0,1]$, $\ell > 0$, *and*

$$\eta = \max\{\beta+\mu, \kappa+\mu, \delta+\mu, \gamma+\upsilon\} \tag{50}$$

for some $\beta, \delta, \kappa, \gamma, \upsilon, \mu \in \mathbb{R}_+$. *If*

$$\frac{\eta\ell^\alpha}{\Gamma(\alpha+1)} < 1 \tag{51}$$

thus, there is a unique solution to the problem in Equations (26)–(27) on $[0, \ell]$.

Proof. Similar to the steps taken to prove Theorem 6, problem in Equations (26)–(27) has already been transformed into fixed-point problem in Equation (31).

Let $\varphi, \omega \in \Omega$, then

$$\begin{aligned}
&\left|\mathcal{T}_i\varphi(t) - \mathcal{T}_i\omega(t)\right| \\
&\leq \frac{1}{\Gamma(\alpha)} \int_0^t (t-\tau)^{\alpha-1} \left|\psi_i(\tau, \varphi(\tau)) - \psi_i(\tau, \omega(\tau))\right| d\tau, \ \forall i \in \overline{1,5}
\end{aligned} \tag{52}$$

For all $t \in [0, \ell]$, we have

$$\begin{aligned}
\left|\psi_1(t, \varphi(t)) - \psi_1(t, \omega(t))\right| &\leq \max\{\beta+\mu, \delta\}\|\varphi-\omega\|_\Omega \\
\left|\psi_2(t, \varphi(t)) - \psi_2(t, \omega(t))\right| &\leq \max\{\beta, \kappa+\mu\}\|\varphi-\omega\|_\Omega \\
\left|\psi_3(t, \varphi(t)) - \psi_3(t, \omega(t))\right| &\leq \max\{\kappa, \delta+\mu\}\|\varphi-\omega\|_\Omega \\
\left|\psi_4(t, \varphi(t)) - \psi_4(t, \omega(t))\right| &\leq (\gamma+\upsilon)\|\varphi-\omega\|_\Omega \\
\left|\psi_5(t, \varphi(t)) - \psi_5(t, \omega(t))\right| &\leq \max\{\gamma, \upsilon\}\|\varphi-\omega\|_\Omega
\end{aligned} \tag{53}$$

Then

$$\left|\psi_i(t, \varphi(t)) - \psi_i(t, \omega(t))\right| \leq \eta\|\varphi-\omega\|_\Omega, \ \forall i \in \overline{1,5} \tag{54}$$

From Equation (52), we find

$$\left\|\mathcal{T}_i\varphi - \mathcal{T}_i\omega\right\|_\infty \leq \frac{\eta\ell^\alpha}{\Gamma(\alpha+1)}\|\varphi-\omega\|_\Omega, \ \forall i \in \overline{1,5} \tag{55}$$

and

$$\|\mathcal{T}\varphi - \mathcal{T}\omega\|_\Omega \leq \frac{\eta\ell^\alpha}{\Gamma(\alpha+1)}\|\varphi-\omega\|_\Omega \tag{56}$$

Referring to Equation (51), $\mathcal{T}$ is considered as a contraction operator. By employing Banach's Contraction Principle, it can be deduced that $\mathcal{T}$ possesses a unique fixed point, which corresponds to the unique solution of the problem in Equations (26)–(27) on $[0, \ell]$.

3.3. Ulam–Hyers Stability for the Normalized Model

Definition 8. *The system of Caputo-type fractional differential equations in Equation (26) is Ulam–Hyers stable if there exists a real number $c > 0$ such that for each $\varepsilon = \max\{\varepsilon_1, \dots, \varepsilon_5\}$ with $\varepsilon_i > 0$, $i \in \overline{1,5}$, and for each solution $\omega \in \Omega$ of the inequality*

$$\left|{}^{C}D^{\alpha}_{0^+}\omega_i(t) - \psi_i(t,\omega(t))\right| \le \varepsilon_i, \quad t \in [0,\ell],\ i \in \overline{1,5} \tag{57}$$

there exists $\varphi \in \Omega$ a solution of (26) with

$$\|\omega - \varphi\|_{\Omega} \le c\varepsilon \tag{58}$$

Definition 9. *The system of Caputo-type fractional differential equations in Equation (26) is generalized Ulam–Hyers stable if there exists $\xi \in C\left(\mathbb{R}_+, \mathbb{R}_+\right)$, $\xi(0) = 0$, such that for each solution $\omega \in \Omega$ of inequality in Equation (57), there exists a solution $\varphi \in \Omega$ of Equation (26) with*

$$\|\omega - \varphi\|_{\Omega} \le \xi(\varepsilon). \tag{59}$$

Remark 10 (Ref. [40]). If $\omega \in \Omega$ is a solution of inequality Equation (57), then there exist $\left(\varepsilon_i\right)_{i\in\overline{1,5}} > 0$ and $\phi \in \Omega$, such that

1) ${}^{C}D^{\alpha}_{0^+}\omega_i(t) = \psi_i(t,\omega(t)) + \phi_i(t)$, $t \in [0,\ell]$, $i \in \overline{1,5}$,
2) $|\phi_i(t)| \le \varepsilon_i$, for all $t \in [0,\ell]$, and each $i \in \overline{1,5}$.

The subsequent lemma aids in establishing the stability of system in Equation (26).

Lemma 11. *If $\omega \in \Omega$ is the solution of inequality in Equation (57), then there exist $\left(\varepsilon_i\right)_{i\in\overline{1,5}} > 0$ such that ω will be the solution of the inequality*

$$\left|\omega_i(t) - \omega_i(0) - \frac{1}{\Gamma(\alpha)}\int_0^t (t-\tau)^{\alpha-1}\psi_i(\tau,\omega(\tau))d\tau\right| \le \frac{\ell^{\alpha}\varepsilon_i}{\Gamma(\alpha+1)} \tag{60}$$

for each $i \in \overline{1,5}$.

Proof. If ω is a solution of Equation (57), we have from Remark 10

$$\begin{cases} {}^{C}D^{\alpha}_{0^+}\omega_i(t) = \psi_i(t,\omega(t)) + \phi_i(t), & t \in [0,\ell],\ i \in \overline{1,5}, \\ |\phi_i(t)| \le \varepsilon_i, & \left(\varepsilon_i\right)_{i\in\overline{1,5}} > 0 \end{cases} \tag{61}$$

hence

$$\omega_i(t) = \omega_i(0) + \frac{1}{\Gamma(\alpha)}\int_0^t (t-\tau)^{\alpha-1}\left[\psi_i(\tau,\omega(\tau)) + \phi_i(\tau)\right]d\tau \tag{62}$$

Also,

$$\begin{aligned} &\left|\omega_i(t) - \omega_i(0) - \frac{1}{\Gamma(\alpha)}\int_0^t (t-\tau)^{\alpha-1}\psi_i(\tau,\omega(\tau))d\tau\right| \\ &= \left|\omega_i(0) + \frac{1}{\Gamma(\alpha)}\int_0^t (t-\tau)^{\alpha-1}\left[\psi_i(\tau,\omega(\tau)) + \phi_i(\tau)\right]d\tau\right. \\ &\quad \left. - \omega_i(0) - \frac{1}{\Gamma(\alpha)}\int_0^t (t-\tau)^{\alpha-1}\psi_i(\tau,\omega(\tau))d\tau\right| \\ &\le \frac{1}{\Gamma(\alpha)}\int_0^t (t-\tau)^{\alpha-1}|\phi_i(\tau)|d\tau \\ &\le \frac{\ell^{\alpha}\varepsilon_i}{\Gamma(\alpha+1)}, \quad \forall i \in \overline{1,5} \end{aligned} \tag{63}$$

That establishes the lemma.

Theorem 12. *Assuming that Equation (51) holds, system in Equation (26) is Ulam–Hyers stable. Furthermore, it can also be asserted that (26) is a generalized Ulam–Hyers stable system.*

Proof. Let $\left(\varepsilon_i\right)_{i\in\overline{1,5}} > 0$, we define $\omega \in \Omega$ as a solution of the inequality

$$\left|{}^{C}D^{\alpha}_{0^+}\omega_i(t) - \psi_i(t,\omega(t))\right| \le \varepsilon_i, \quad t \in [0,\ell],\ i \in \overline{1,5} \tag{64}$$

and $\varphi \in \Omega$ is the unique solution of system in Equation (26) with the conditions

$$\varphi_i(0) = \omega_i(0), \quad \forall i \in \overline{1,5} \tag{65}$$

Then

$$\varphi_i(t) = \omega_i(0) + \frac{1}{\Gamma(\alpha)}\int_0^t (t-\tau)^{\alpha-1}\psi_i(\tau,\varphi(\tau))d\tau \tag{66}$$

and

$$\begin{aligned} |\omega_i(t) - \varphi_i(t)| &= \left|\omega_i(t) - \omega_i(0) - \frac{1}{\Gamma(\alpha)}\int_0^t (t-\tau)^{\alpha-1}\psi_i(\tau,\varphi(\tau))d\tau\right| \\ &\le \left|\omega_i(t) - \omega_i(0) - \frac{1}{\Gamma(\alpha)}\int_0^t (t-\tau)^{\alpha-1}\psi_i(\tau,\omega(\tau))d\tau\right| \\ &\quad + \frac{1}{\Gamma(\alpha)}\int_0^t (t-\tau)^{\alpha-1}|\psi_i(\tau,\omega(\tau)) - \psi_i(\tau,\varphi(\tau))|d\tau \end{aligned} \tag{67}$$

Using Equation (54), and Lemma 11, we get

$$\begin{aligned} &|\omega_i(t) - \varphi_i(t)| \\ &\le \frac{\ell^{\alpha}}{\Gamma(\alpha+1)}\left(\varepsilon_i + \eta\|\varphi - \omega\|_{\Omega}\right), \quad \forall t \in [0,\ell],\ \forall i \in \overline{1,5} \end{aligned} \tag{68}$$

Taking the maximum from both sides, we obtain

$$\|\varphi - \omega\|_{\Omega} \le \frac{\ell^{\alpha}}{\Gamma(\alpha+1)}\left(\varepsilon + \eta\|\varphi - \omega\|_{\Omega}\right) \tag{69}$$

Thus

$$\|\varphi - \omega\|_{\Omega} \le c\varepsilon, \tag{70}$$

where $c = \frac{\ell^{\alpha}}{\Gamma(\alpha+1) - \eta\ell^{\alpha}}$. This implies that system in Equation (26) is stable in the Ulam–Hyers sense and is consequently generalized Ulam–Hyers stable if we set $\xi(t) = ct$.

4. Analysis for the Fractional SIP(H)–SI(M) Model

4.1. Basic Reproduction Number and Equilibrium Points

In this section, the basic reproduction number of the system in Equation (22) is calculated using the next-generation matrix method. Denoted as $\mathfrak{R}_0$, which signifies the average number of secondary infections resulting from the introduction of a single infection into the susceptible population. This can be calculated as the spectral radius of the $\mathcal{Y}\mathcal{Z}^{-1}$ matrix.

Theorem 13. *The basic reproduction number of system in Equation (22) is determined by*

$$\mathfrak{R}_0 = \sqrt{\frac{\beta\gamma\lambda\Lambda}{\upsilon^2\mu(\kappa+\mu)}} \tag{71}$$

Proof. Because the SIP(H)–SI(M) model is composed of infection components I, P, and F, we obtain:

$$\gamma_i - z_i = \begin{pmatrix} \beta F(t)S(t) - (\kappa+\mu)I(t) \\ \kappa I(t) - (\delta+\mu)P(t) \\ \gamma I(t)V(t) - \upsilon F(t) \end{pmatrix} \tag{72}$$

Accordingly,

$$\gamma_i = \begin{pmatrix} \beta F(t)S(t) \\ 0 \\ \gamma I(t)V(t) \end{pmatrix}, z_i = \begin{pmatrix} (\kappa+\mu)I(t) \\ (\delta+\mu)P(t) - \kappa I(t) \\ \upsilon F(t) \end{pmatrix} \tag{73}$$

Here, γ_i denotes the rate of new infections appearing in compartment i, and z_i denotes the rate of transitions between compartment i and other infected compartments for each $i \in \{1, 2, 3\}$. The new infection matrix $\mathcal{Y}$ and transition matrix $\mathcal{Z}$ are assessed at the disease-free equilibrium point E_1 (Theorem 14), as follows:

$$\mathcal{Y} = \begin{pmatrix} 0 & 0 & \beta S_1^* \\ 0 & 0 & 0 \\ \gamma V_1^* & 0 & 0 \end{pmatrix}, \quad \mathcal{Z} = \begin{pmatrix} \kappa+\mu & 0 & 0 \\ -\kappa & \delta+\mu & 0 \\ 0 & 0 & \upsilon \end{pmatrix} \tag{74}$$

Following the next-generation matrix principle, the basic reproduction number is defined as the spectral radius of matrix $\mathcal{Y}\mathcal{Z}^{-1}$ and is given by Equation (71).

The initial step in comprehending a differential equation is to identify equilibrium points. In epidemiology, we are concerned with two types of equilibrium point:

1) Disease-free equilibrium is defined as the point at which no disease (or death from disease) is introduced into the population and is depicted in the model as $I = P = F = 0$.
2) Other equilibrium points, where $I \neq 0$ and $F \neq 0$, are indicated as endemic equilibrium points (or outbreak equilibrium points).

We define the positive real values

$$m_1 = \kappa + \mu, \qquad m_2 = \delta + \mu \tag{75}$$

to facilitate the calculations and establish the following theorem.

Theorem 14. *The system in Equation (22) has two types of equilibrium points*

1) *Disease-free equilibrium*

$$E_1 = \left(S_1^*, I_1^*, P_1^*, V_1^*, F_1^*\right) = \left(\frac{\Lambda}{\mu}, 0, 0, \frac{\lambda}{\upsilon}, 0\right) \tag{76}$$

2) *Endemic equilibrium point* $E_2 = \left(S_2^*, I_2^*, P_2^*, V_2^*, F_2^*\right)$, *which is*

$$E_2 = \left(S_1^*\left(1 - \frac{\mu(\delta+m_1)}{\Lambda m_2}I_2^*\right), I_2^*, \frac{\kappa}{m_2}I_2^*, \frac{\lambda}{\gamma I_2^* + \upsilon}, \frac{\gamma\lambda I_2^*}{\upsilon(\gamma I_2^* + \upsilon)}\right) \tag{77}$$

where

$$I_2^* = \frac{m_1 m_2 \upsilon^2}{\gamma\left[m_1 m_2 \upsilon + \beta\lambda(\delta+m_1)\right]}\left(\mathfrak{R}_0^2 - 1\right) \tag{78}$$

The existence of the endemic equilibrium point depends on $\mathfrak{R}_0 > 1$.

Proof. To determine the equilibrium points for system in Equation (22), we set ${}^{C}\mathcal{D}_{0^+}^{\alpha}\varphi(t) = \vec{0}$, with $\varphi = (S, I, P, V, F)$. Therefore

$$\begin{cases} 0 = \Lambda + \delta P(t) - (\beta F(t) + \mu)S(t) & (eq1) \\ 0 = \beta F(t)S(t) - (\kappa+\mu)I(t) & (eq2) \\ 0 = \kappa I(t) - (\delta+\mu)P(t) & (eq3) \\ 0 = \lambda - (\gamma I(t) + \upsilon)V(t) & (eq4) \\ 0 = \gamma I(t)V(t) - \upsilon F(t) & (eq5) \end{cases} \tag{79}$$

From equations $(eq3)$ and $(eq4)$, we have

$$P(t) = \frac{\kappa}{m_2}I(t) \quad \text{and} \quad V(t) = \frac{\lambda}{\gamma I(t) + \upsilon} \tag{80}$$

Substituting the expression of $V(t)$ in equation $(eq5)$, we get

$$F(t) = \frac{\gamma\lambda I(t)}{\upsilon(\gamma I(t) + \upsilon)} \tag{81}$$

If we add $(eq1)$ to $(eq2)$ we obtain

$$S(t) = S_1^*\left(1 - \frac{\mu(\delta+m_1)}{\Lambda m_2}I(t)\right) \tag{82}$$

1) If $I = 0$, we can easily obtain the first disease-free equilibrium point E_1.
2) When $I \neq 0$, equation $(eq2)$ gives us

$$I_2^* = \frac{m_1 m_2 \upsilon^2}{\gamma\left[m_1 m_2 \upsilon + \beta\lambda(\delta+m_1)\right]}\left(\mathfrak{R}_0^2 - 1\right) \tag{83}$$

Consequently, we obtain the required endemic equilibrium point E_2, which exists for $\mathfrak{R}_0 > 1$.

Hence, the theorem is proved.

4.2. Stability Study of Disease-Free Equilibrium Point

4.2.1. Local Stability Analysis of E_1

Theorem 15. *The disease-free equilibrium point of system in Equation (22) is locally asymptotically stable when* $\mathfrak{R}_0 < 1$.

Proof. The Jacobian matrix for system in Equation (22) is written as follows

$$J = \begin{pmatrix} \frac{\partial \psi_1}{\partial S} & \frac{\partial \psi_1}{\partial I} & \frac{\partial \psi_1}{\partial P} & \frac{\partial \psi_1}{\partial V} & \frac{\partial \psi_1}{\partial F} \\ \frac{\partial \psi_2}{\partial S} & \frac{\partial \psi_2}{\partial I} & \frac{\partial \psi_2}{\partial P} & \frac{\partial \psi_2}{\partial V} & \frac{\partial \psi_2}{\partial F} \\ \frac{\partial \psi_3}{\partial S} & \frac{\partial \psi_3}{\partial I} & \frac{\partial \psi_3}{\partial P} & \frac{\partial \psi_3}{\partial V} & \frac{\partial \psi_3}{\partial F} \\ \frac{\partial \psi_4}{\partial S} & \frac{\partial \psi_4}{\partial I} & \frac{\partial \psi_4}{\partial P} & \frac{\partial \psi_4}{\partial V} & \frac{\partial \psi_4}{\partial F} \\ \frac{\partial \psi_5}{\partial S} & \frac{\partial \psi_5}{\partial I} & \frac{\partial \psi_5}{\partial P} & \frac{\partial \psi_5}{\partial V} & \frac{\partial \psi_5}{\partial F} \end{pmatrix} \tag{84}$$

where $\psi_{1\le i\le 5}(t, \varphi(t))$ represents the right-hand side of Equation (22). Then

$$J = \begin{pmatrix} -(\beta F + \mu) & 0 & \delta & 0 & -\beta S \\ \beta F & -m_1 & 0 & 0 & \beta S \\ 0 & \kappa & -m_2 & 0 & 0 \\ 0 & -\gamma V & 0 & -(\gamma I + \upsilon) & 0 \\ 0 & \gamma V & 0 & \gamma I & -\upsilon \end{pmatrix} \tag{85}$$

The eigenvalues of $J(E_1)$ are given as the roots of the following characteristic polynomial

$$f_1(X) = -(\mu + X)(m_2 + X)(\upsilon + X) \times \left[X^2 + (m_1 + \upsilon)X + m_1\upsilon(1 - \mathfrak{R}_0^2)\right] \tag{86}$$

The roots of $f_1(X)$ are negative reals or complexes of negative real parts, which makes E_1 locally asymptotically stable.

4.2.2. Global Stability Analysis of E_1

Theorem 16. *The disease-free equilibrium point E_1 of system in Equation (22) is globally asymptotically stable if* $\mathfrak{R}_0 < 1$.

Proof. To prove the theorem, we examine the following Lyapunov function

$$W(S, I, P, V, F) = c_1 I + c_2 P + c_3 F \tag{87}$$

We consider c_i to be positive constants for $i \in 1, 2, 3$, to be determined later. The fractional derivative of W along with the solution of system in Equation (22) is calculated as follows:

$$\begin{aligned} {}^{C}\mathcal{D}^{\alpha}_{0^+} W &= c_1\, {}^{C}\mathcal{D}^{\alpha}_{0^+} I + c_2\, {}^{C}\mathcal{D}^{\alpha}_{0^+} P + c_3\, {}^{C}\mathcal{D}^{\alpha}_{0^+} F \\ &= c_1[\beta FS - (\kappa + \mu)I] + c_2[\kappa I - (\delta + \mu)P] + c_3[\gamma IV - \upsilon F] \\ &\le c_1\left[\frac{\beta\Lambda}{\mu}F - (\kappa + \mu)I\right] + c_2[\kappa I - (\delta + \mu)P] + c_3\left[\frac{\gamma\lambda}{\upsilon}I - \upsilon F\right] \\ &= \left[-c_1(\kappa + \mu) + c_2\kappa + c_3\frac{\gamma\lambda}{\upsilon}\right]I - c_2(\delta + \mu)P + \left[c_1\frac{\beta\Lambda}{\mu} - c_3\upsilon\right]F \end{aligned} \tag{88}$$

By choosing $c_1 = \upsilon$, $c_2 = 0$, and $c_3 = \frac{\beta\Lambda}{\mu}$, we obtain

$${}^{C}\mathcal{D}^{\alpha}_{0^+} W \le \upsilon(\kappa + \mu)\left(\mathfrak{R}_0^2 - 1\right)I \tag{89}$$

Thus, if $\mathfrak{R}_0 < 1$, we get ${}^{C}\mathcal{D}^{\alpha}_{0^+} W \le 0$, then $\frac{dW}{dt} < 0$. According to LaSalle's invariance principle,[41] this implies that E_1 is globally asymptotically stable.

4.3. Stability Study of Endemic Equilibrium Point

4.3.1. Local Stability Analysis of E_2

Let g_0, g_1, and g_2, be such that

$$\begin{aligned} g_0 &= \left(\gamma I_2^* + \upsilon\right)\left(\frac{\kappa\delta + (m_1 + \delta)(\beta F_2^* + \mu)}{m_2}\right) \\ g_1 &= m_1\left(\gamma I_2^* + \upsilon\right) + \frac{\begin{matrix}\beta F_2^*\left[\delta\mu + m_1\left(\gamma I_2^* + \upsilon + \mu\right) + m_2\left(\gamma I_2^* + \upsilon\right)\right] \\ +\mu m_2\left(m_1 + \gamma I_2^* + \upsilon\right)\end{matrix}}{\mu + m_2} \\ g_2 &= \left(\beta F_2^* + \mu\right)m_2 + \left(m_1 + \gamma I_2^* + \upsilon\right)\left(\beta F_2^* + \mu + m_2\right) \\ &\quad + m_1\left(\gamma I_2^* + \upsilon\right) \end{aligned} \tag{90}$$

Theorem 17. *If we put*

$$\beta\gamma V_2^* S_2^* < \min\{g_0, g_1, g_2\} \tag{91}$$

the endemic equilibrium point E_2 of system in Equation (22) is locally asymptotically stable when $\mathfrak{R}_0 > 1$.

Proof. As shown in the previous section, the Jacobian matrix $J(E_2)$ for Equation (22) is

$$J_{E_2} = \begin{pmatrix} -(\beta F_2^* + \mu) & 0 & \delta & 0 & -\beta S_2^* \\ \beta F_2^* & -m_1 & 0 & 0 & \beta S_2^* \\ 0 & \kappa & -m_2 & 0 & 0 \\ 0 & -\gamma V_2^* & 0 & -(\gamma I_2^* + \upsilon) & 0 \\ 0 & \gamma V_2^* & 0 & \gamma I_2^* & -\upsilon \end{pmatrix} \tag{92}$$

The characteristic polynomial is given by

$$f_2(X) = -(\upsilon + X)\left(X^4 + a_3X^3 + a_2X^2 + a_1X + a_0\right) \tag{93}$$

where

$$\begin{aligned} a_0 &= \mu m_2\left(g_0 - \beta\gamma V_2^* S_2^*\right) \\ a_1 &= \left(m_2 + \mu\right)\left(g_1 - \beta\gamma V_2^* S_2^*\right) \\ a_2 &= g_2 - \beta\gamma V_2^* S_2^* \\ a_3 &= \beta F_2^* + \gamma I_2^* + m_1 + m_2 + \mu + \upsilon \end{aligned} \tag{94}$$

According to Descartes' rule, the roots of $f_2(X)$ are negative reals or complexes of negative real parts. Therefore, the required result is obtained.

4.3.2. Global Stability Analysis of E_2

From system in Equation (22), we obtain

$$\begin{cases} \Lambda = -\delta P_2^* + \left(\beta F_2^* + \mu\right) S_2^* \\ (\kappa + \mu) I_2^* = \beta S_2^* F_2^* \\ (\delta + \mu) P_2^* = \kappa I_2^* \\ \lambda = \left(\gamma I_2^* + \upsilon\right) V_2^* \\ \upsilon F_2^* = \gamma I_2^* V_2^* \end{cases} \tag{95}$$

Theorem 18. *Suppose that*

$$\frac{P^*}{P} \le 1 \le \min\left\{ \left(\frac{S^*}{S} - 1\right)^2 + \frac{FI^*}{F^*I}, \left(\frac{V^*}{V} - 1\right)^2 + \frac{FI^*}{F^*I} \right\} \tag{96}$$

Therefore, the endemic equilibrium point E_2 of the system in Equation (22) is globally asymptotically stable when $\Re_0 > 1$.

Proof. We analyze the following nonlinear Lyapunov function of the Goh-Volterra form:

$$\begin{aligned} W(S, I, P, V, F) = & \left[S(t) - S^* - S^* \log \frac{S(t)}{S^*}\right] \\ & + \left[I(t) - I^* - I^* \log \frac{I(t)}{I^*}\right] \\ & + \frac{\delta}{\delta + \mu}\left[P(t) - P^* - P^* \log \frac{P(t)}{P^*}\right] \\ & + \frac{\beta S^*}{\upsilon}\left[V(t) - V^* - V^* \log \frac{V(t)}{V^*}\right] \\ & + \frac{\beta S^*}{\upsilon}\left[F(t) - F^* - F^* \log \frac{F(t)}{F^*}\right] \end{aligned} \tag{97}$$

By leveraging the findings on Volterra-type Lyapunov functions for fractional-order epidemic systems outlined in ref. [42], and subsequently employing the Caputo derivative on both sides, the following inequality can be established:

$$\begin{aligned} {}^C\mathcal{D}^{\alpha}_{0^+} W \le & \left(1 - \frac{S^*}{S}\right) {}^C\mathcal{D}^{\alpha}_{0^+} S(t) + \left(1 - \frac{I^*}{I}\right) {}^C\mathcal{D}^{\alpha}_{0^+} I(t) \\ & + \frac{\delta}{\delta + \mu}\left(1 - \frac{P^*}{P}\right) {}^C\mathcal{D}^{\alpha}_{0^+} P(t) \\ & + \frac{\beta S^*}{\upsilon}\left(1 - \frac{V^*}{V}\right) {}^C\mathcal{D}^{\alpha}_{0^+} V(t) + \frac{\beta S^*}{\upsilon}\left(1 - \frac{F^*}{F}\right) {}^C\mathcal{D}^{\alpha}_{0^+} F(t) \end{aligned} \tag{98}$$

A simple calculation provides the following result

$$\begin{aligned} \left(1 - \frac{S^*}{S}\right) {}^C\mathcal{D}^{\alpha}_{0^+} S &= \left(1 - \frac{S^*}{S}\right)[\Lambda + \delta P - (\beta F + \mu) S] \\ &= \left(1 - \frac{S^*}{S}\right)[-\delta P^* + (\beta F^* + \mu) S^* \\ &\quad + \delta P - (\beta F + \mu) S] \\ &= \mu S^*\left(2 - \frac{S^*}{S} - \frac{S}{S^*}\right) + \beta F^* S^*\left(1 - \frac{S^*}{S}\right) \\ &\quad - \beta FS + \delta P - \delta P^* \\ &\quad + \beta FS^* - \delta P \frac{S^*}{S} + \delta P^* \frac{S^*}{S} \end{aligned} \tag{99}$$

In same way, we find

$$\begin{aligned} \left(1 - \frac{I^*}{I}\right) {}^C\mathcal{D}^{\alpha}_{0^+} I &= \left(1 - \frac{I^*}{I}\right)[\beta FS - (\kappa + \mu) I] \\ &= \beta FS - (\kappa + \mu) I - \beta FS \frac{I^*}{I} + (\kappa + \mu) I^*. \end{aligned} \tag{100}$$

Next

$$\begin{aligned} \frac{\delta}{\delta + \mu}\left(1 - \frac{P^*}{P}\right) {}^C\mathcal{D}^{\alpha}_{0^+} P &= \frac{\delta}{\delta + \mu}\left(1 - \frac{P^*}{P}\right)[\kappa I - (\delta + \mu) P] \\ &= \delta P^* - \delta P + \frac{\delta \kappa}{\delta + \mu} I - \frac{\delta \kappa}{\delta + \mu} I \frac{P^*}{P} \end{aligned} \tag{101}$$

Also

$$\begin{aligned} \frac{\beta S^*}{\upsilon}\left(1 - \frac{V^*}{V}\right) {}^C\mathcal{D}^{\alpha}_{0^+} V &= \frac{\beta S^*}{\upsilon}\left(1 - \frac{V^*}{V}\right)[\lambda - (\gamma I + \upsilon) V] \\ &= \frac{\beta S^*}{\upsilon}\left(1 - \frac{V^*}{V}\right)[(\gamma I^* + \upsilon) V^* - (\gamma I + \upsilon) V] \\ &= \beta S^* V^*\left(2 - \frac{V^*}{V} - \frac{V}{V^*}\right) + \frac{\beta S^*}{\upsilon} \gamma I^* V^* \\ &\quad - \frac{\beta S^*}{\upsilon} \gamma IV + \frac{\beta S^*}{\upsilon} \gamma IV^* - \frac{\beta S^*}{\upsilon} \gamma I^* V^* \frac{V^*}{V} \end{aligned} \tag{102}$$

and

$$\begin{aligned} \frac{\beta S^*}{\upsilon}\left(1 - \frac{F^*}{F}\right) {}^C\mathcal{D}^{\alpha}_{0^+} F &= \frac{\beta S^*}{\upsilon}\left(1 - \frac{F^*}{F}\right)[\gamma IV - \upsilon F] \\ &= \frac{\beta S^*}{\upsilon} \gamma IV - \beta S^* F - \frac{\beta S^*}{\upsilon} \gamma IV \frac{F^*}{F} + \beta S^* F^* \end{aligned} \tag{103}$$

Then

$$\begin{aligned} {}^C\mathcal{D}^{\alpha}_{0^+} W \le & \mu S^*\left(2 - \frac{S^*}{S} - \frac{S}{S^*}\right) \\ & + \beta F^* S^*\left(4 - \frac{S^*}{S} - \frac{V^*}{V} - \frac{IVF^*}{I^* V^* F} - \frac{FSI^*}{F^* S^* I}\right) \\ & + \beta S^* V^*\left(2 - \frac{V^*}{V} - \frac{V}{V^*}\right) \\ & + \delta P^*\left(\frac{S^*}{S} - \frac{S^* P}{SP^*} - \frac{P^* I}{PI^*} + \frac{I}{I^*}\right) \end{aligned} \tag{104}$$

with

$$\begin{cases} 2-\frac{S^*}{S}-\frac{S}{S^*}\le 0 \\ \quad \text{and} \quad 2-\frac{V^*}{V}-\frac{V}{V^*}\le 0 \\ \frac{S^*}{S}-\frac{S^*P}{SP^*}-\frac{P^*I}{PI^*}+\frac{I}{I^*}\le 0 \\ \quad \text{for} \quad \frac{P^*}{P}\le 1 \\ 4-\frac{S^*}{S}-\frac{V^*}{V}-\frac{IVF^*}{I^*V^*F}-\frac{FSI^*}{F^*S^*I}\le 0 \\ \quad \text{for} \quad \min\left\{\left(\frac{S^*}{S}-1\right)^2+\frac{FI^*}{F^*I},\left(\frac{V^*}{V}-1\right)^2+\frac{FI^*}{F^*I}\right\}\ge 1 \end{cases} \tag{105}$$

Because all parameters are nonnegative, we obtain ${}^{C}\mathcal{D}^{\alpha}_{0^+}W\le 0$, which follows that $\frac{dW}{dt}\le 0$ when $\Re_0>1$. According to LaSalle's invariance principle,[41] $(S,I,P,V,F)\to(S^*,I^*,P^*,V^*,F^*)$ as $t\to\infty$.

5. Data Fitting Analysis through Numerical Simulation

In this section, we validate our analytical findings by determining specific parameter values and using the Adams-type predictor-corrector method[43,44] to perform a numerical simulation of the proposed nonlinear system in Equation (1) to obtain an approximate solution for the model.

The *nlinfit* function in MATLAB is a powerful tool for nonlinear regressions. It is used to model predictive relationships between variables when the data or the relationship between variables is complex and does not fit simple linear models. It also provides a convenient interface for data-fitting problems.

Using this tool, we identified the parameter values closest to those in **Table 2**, resulting in a minimum error for the fractional-order model. These estimated parameters were then incorporated into the fractional-order SIP(H)–SI(M) model (1). To ensure consistent physical dimensions, we modified the units of all model parameters to align with the dimension $(time)^{-\alpha}$, which corresponds to the fractional derivatives with dimension (order α).

5.1. Numerical Scheme for the Fractional SIP(H)–SI(M) Model

In this subsection, we outline the generalized predictor-corrector scheme associated with the Adams–Bashforth–Moulton algorithm,[45] which can be used to solve fractional epidemic systems. The chosen method is stable, converges faster, and has superior accuracy compared to other methods,[44–46] making it an optimal choice for our SIP(H)–SI(M) model (1).

Consider the following Cauchy problem of Caputo fractional derivative of order $\alpha>0$

$$\begin{aligned} &{}^{C}\mathcal{D}^{\alpha}_{0^+}\varphi(t)=\psi(t,\varphi(t)), && 0\le t\le \ell, \quad \alpha\in(m-1,m] \\ &\varphi^{(k)}(0)=\varphi_0^{(k)}, && k=0,1,\dots,m-1, \quad m\in\mathbb{N} \end{aligned} \tag{106}$$

where ψ is a nonlinear function. The Cauchy problem is equivalent to the Volterra integral equation:

$$\varphi(t)=\sum_{k=0}^{m-1}\frac{t^k}{k!}\varphi_0^{(k)}+\frac{1}{\Gamma(\alpha)}\int_0^t(t-\tau)^{\alpha-1}\psi(\tau,\varphi(\tau))d\tau \tag{107}$$

Consider a uniform grid $\{t_n=nh,\ \text{with}\ n=0,1,\dots,L\}$ for some integer L and $h=\frac{\ell}{L}$. Let $\varphi_h(t_n)$ denote the approximation of $\varphi(t_n)$. Assume that we have already calculated approximations $\varphi_h(t_j)$, for $j=1,2,\dots,n$, and we want to obtain $\varphi_h(t_{n+1})$ using Equation (107).

$$\begin{aligned} \varphi_h(t_{n+1})=&\sum_{k=0}^{m-1}\frac{t_{n+1}^k}{k!}\varphi_0^{(k)}+\frac{h^\alpha}{\Gamma(\alpha+2)}\psi\left(t_{n+1},\varphi_h^{pr}(t_{n+1})\right) \\ &+\frac{h^\alpha}{\Gamma(\alpha+2)}\sum_{j=0}^{n}a_{j,n+1}\psi\left(t_j\varphi_h(t_j)\right) \end{aligned} \tag{108}$$

where

$$\alpha_{j,n+1}=\begin{cases} n^{\alpha+1}-(n-\alpha)(n+1)^\alpha & \\ \qquad\qquad \text{if } j=0 & \\ (n-j+2)^{\alpha+1}+(n-j)^{\alpha+1}-2(n-j+1)^{\alpha+1} & \\ \qquad\qquad \text{if } 1\le j\le n & \\ 1 & \\ \qquad\qquad \text{if } j=n+1 & \end{cases} \tag{109}$$

The preliminary approximation $\varphi_h^{pr}(t_{n+1})$ is called predictor and is given by

$$\varphi_h^{pr}(t_{n+1})=\sum_{k=0}^{m-1}\frac{t_{n+1}^k}{k!}\varphi_0^{(k)}+\frac{1}{\Gamma(\alpha)}\sum_{j=0}^{n}b_{j,n+1}\psi\left(t_j,\varphi_h(t_j)\right) \tag{110}$$

with

$$b_{j,n+1}=\frac{h^\alpha}{\alpha}\left[(n+1-j)^\alpha-(n-j)^\alpha\right] \tag{111}$$

Error in this method is

$$\max_{n=0,1,\dots,L}\left|\varphi(t_n)-\varphi_h(t_n)\right|=O(h^\Theta) \tag{112}$$

where $\Theta=\min(2,1+\alpha)$. Consequently, by taking $\varphi_h(t_n)=\left(S_{H_n},I_{H_n},P_{H_n},S_{M_n},I_{M_n}\right)$ and

$$\begin{aligned} \psi\left(t_n,\varphi_h(t_n)\right)=&\Big(\psi_1\left(t_n,\varphi_h(t_n)\right),\psi_2\left(t_n,\varphi_h(t_n)\right),\psi_3\left(t_n,\varphi_h(t_n)\right), \\ &\psi_4\left(t_n,\varphi_h(t_n)\right),\psi_5\left(t_n,\varphi_h(t_n)\right)\Big) \end{aligned} \tag{113}$$

where $(\psi_i)_{1\le i\le 5}$ satisfy Equation (25). We explore the numerical scheme corresponding to the SIP(H)–SI(M) model (1):

$$S_{H_{n+1}} = S_{H_0} + \frac{h^\alpha}{\Gamma(\alpha+2)}\left(\Lambda H - \left(\frac{\beta I^{pr}_{M_{n+1}}}{M} + \mu\right) S^{pr}_{H_{n+1}} + \delta R^{pr}_{H_{n+1}}\right) + \frac{h^\alpha}{\Gamma(\alpha+2)} \sum_{j=0}^{n} a_{j,n+1}\left(\Lambda H - \left(\frac{\beta I_{M_j}}{M} + \mu\right) S_{H_j} + \delta R_{H_j}\right)$$

$$I_{H_{n+1}} = E_{H_0} + \frac{h^\alpha}{\Gamma(\alpha+2)}\left(\frac{\beta I^{pr}_{M_{n+1}}}{M} S^{pr}_{H-n+1} - (\kappa+\mu) I^{pr}_{H_{n+1}}\right) + \frac{h^\alpha}{\Gamma(\alpha+2)} \sum_{j=0}^{n} a_{j,n+1}\left(\frac{\beta I_{M_j}}{M} S_{H_j} - (\kappa+\mu) I_{H_j}\right)$$

$$P_{H_{n+1}} = P_{H_0} + \frac{h^\alpha}{\Gamma(\alpha+2)}\left(\kappa I^{pr}_{H_{n+1}} - (\delta+\mu) R^{pr}_{H_{n+1}}\right) + \frac{h^\alpha}{\Gamma(\alpha+2)} \sum_{j=0}^{n} a_{j,n+1}\left(\kappa I_{H_j} - (\delta+\mu) R_{H_j}\right)$$

$$S_{M_{n+1}} = S_{M_0} + \frac{h^\alpha}{\Gamma(\alpha+2)}\left(\lambda M - \left(\frac{\gamma I^{pr}_{H_{n+1}}}{H} + \upsilon\right) S^{pr}_{M_{n+1}}\right) + \frac{h^\alpha}{\Gamma(\alpha+2)} \sum_{j=0}^{n} a_{j,n+1}\left(\lambda M - \left(\frac{\gamma I_{H_j}}{H} + \upsilon\right) S_{M_j}\right)$$

$$I_{M_{n+1}} = I_{M_0} + \frac{h^\alpha}{\Gamma(\alpha+2)}\left(\frac{\gamma I^{pr}_{H_{n+1}}}{H} S^{pr}_{M_{n+1}} - \upsilon I^{pr}_{M_{n+1}}\right) + \frac{h^\alpha}{\Gamma(\alpha+2)} \sum_{j=0}^{n} a_{j,n+1}\left(\frac{\gamma I_{H_j}}{H} S_{M_j} - \upsilon I_{M_j}\right)$$

where $a_{j,n+1}$ are given by Equation (109). Similarly, the predicted values are

$$S^{pr}_{H_{n+1}} = S_{H_0} + \frac{1}{\Gamma(\alpha)} \sum_{j=0}^{n} b_{j,n+1}\left(\Lambda H - \left(\frac{\beta I_{M_j}}{M} + \mu\right) S_{H_j} + \delta R_{H_j}\right)$$

$$I^{pr}_{H_{n+1}} = I_{H_0} + \frac{1}{\Gamma(\alpha)} \sum_{j=0}^{n} b_{j,n+1}\left(\frac{\beta I_{M_j}}{M} S_{H_j} - (\kappa+\mu) I_{H_j}\right)$$

$$P^{pr}_{H_{n+1}} = C_0 + \frac{1}{\Gamma(\alpha)} \sum_{j=0}^{n} b_{j,n+1}\left(\kappa I_{H_j} - (\delta+\mu) P_{H_j}\right)$$

$$S^{pr}_{M_{n+1}} = S_{M_0} + \frac{1}{\Gamma(\alpha)} \sum_{j=0}^{n} b_{j,n+1}\left(\lambda M - \left(\frac{I_{H_j}}{H} + \upsilon\right) S_{M_j}\right)$$

$$I^{pr}_{M_{n+1}} = I_{M_0} + \frac{1}{\Gamma(\alpha)} \sum_{j=0}^{n} b_{j,n+1}\left(\frac{I_{H_j}}{H} S_{M_j} - \upsilon I_{M_j}\right)$$

where $b_{j,n+1}$ are given by Equation (111).

5.2. Fitted Data Analysis of Malaria in Algeria

This section presents a numerical study to contribute to a comprehensive understanding and effective management of malaria in Algeria using data from reliable health sources. Statistical and graphical methods were employed to examine the key epidemiological indicators and provide insights into the malaria situation in the country.

The total population of Algeria was $H = 30\,774\,621$ in 2000.[47] Initial reported malaria cases $I_H(0) = 541$ from the World Health Organization.[48]

In our study, we assume that the total population H remains constant; however, a significant increase in population was observed from 2000 to 2021. Therefore, we cannot directly compare the infection rate in 2000, where there were 541 cases out of a population of 30 774 621, to the infection rate in 2021, where there were 1 164 cases out of a population of 44 177 969. To ensure accuracy, we will adjust the infection rate for each year based on the initial total population in 2000 (**Table 1**), enabling a precise comparison of infection rates over time. Based on these considerations, we will calculate the average recruitment and natural death rates for the entire period from 2000 to 2021.[49]

Lemma 5 ensures that the population does not exceed a specified limit. This constraint is integral to maintaining the validity of our model, as it reflects real-world limitations on population growth and size. Indeed, we have

$$H_0 = H_{2000} = 30\,774\,621 \text{ and } H(t) \le H_{2021} = 44\,177\,969 \quad (114)$$

Subsequently, it must hold that:

$$H_{2021} \le H_{2000} \exp\left(\frac{\Lambda \ell^\alpha}{\Gamma(\alpha+1)}\right) \le \min\left\{H_{2000} \times \exp\left(\frac{0.022818 \ell^\alpha}{\Gamma(\alpha+1)}\right)\right\} \quad (115)$$

Our numerical simulation shows that the greatest value that ℓ can take is 36 when we select $0.79 \le \alpha \le 1$. This decision makes the existence and uniqueness of the solution for the SIP(H)–SI(M) model on $[0, \ell]$ more evident. As a result, H should not be greater than 4.67×10^7, in accordance with the limitations of Lemma 5.

Figure 2 shows the simulation of the model predictions for real-world malaria cases. The predicted parameter values, biological descriptions, and pertinent references are displayed in the table below.

The basic reproduction number in this case is:

$$\mathfrak{R}_0 \simeq 0.4203 < 1 \quad (116)$$

Moreover, following Theorem 7, if we choose $0.79 \le \alpha \le 1$, then SIP(H)–SI(M) model admits a unique solution on $[0, \ell]$, with

$$\ell < 1.8083 \text{ (unit)} \quad (117)$$

As malaria statistics are collected annually or over several months, we chose a unit of 20 years. In this context, the value of ℓ should not exceed 36 years.

Figure 2 presents a chronological table spanning 21 years (beginning in 2000) of confirmed malaria cases. This illustrates fluctuations in the number of infections, reflecting variations in the symptoms and disease severity. Additionally, the data revealed a notable increase in cases coinciding with the emergence of COVID-19.

In the context of Caputo's model, various values of α are examined to represent different scenarios or conditions. **Figures 3** and 4 illustrate the simulation findings with the numerical

Table 1. Adjusted parameters and initial data of infected population in Algeria from 2000 to 2021.

Interpretation	Ref.	2000	2001	⋯	2019	2020	2021	Average
Population of Algeria	[47]	30 774 621	31 200 985	⋯	42 705 368	43 451 666	44 177 969	—
Initial malaria cases	[48]	541	435	⋯	1 014	2 726	1 164	—
Adjusted malaria cases	—	541	429	⋯	731	1 931	811	—
Recruitment rate Λ	[49]	0.0196	0.0193	⋯	0.0233	0.0224	0.0215	0.022818
Natural death rate μ	[49]	0.005	0.0049	⋯	0.0044	0.0054	0.0045	0.0046818

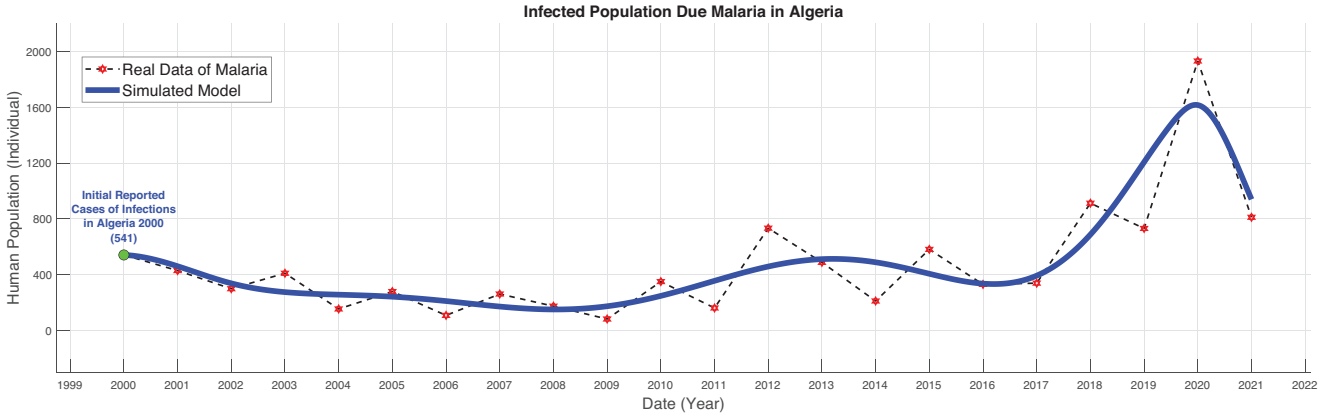

Figure 2. The reported cases of malaria in Algeria (shown with red markers) compared to the predicted cumulative infected cases provided by the proposed model (represented by blue line) for $\alpha = 0.79$.

results employed to analyze the dynamics of two human classes and two categories of mosquitoes.

It is essential to note that the SIP(H) model assumes a well-mixed population, homogeneous mixing, and constant parameters over time. However, it may not fully capture all aspects of disease transmission such as birth, death, or variations in immunity. Furthermore, the suitability of the SIP(H) model varies depending on the specific disease being modeled and the context of the outbreak.

Next, we demonstrate the behavior of the fractional system in Equation (1) using four specific values of $\alpha \in (0, 1]$. The simulation results of the model are presented in **Figure 5**, showing the dynamics of both human and mosquito populations over time for various values of α.

The first graph shows the susceptible human populations from 2000 to 2020. As the parameter α increases, the decline in the susceptible population accelerates, signifying a more rapid spread of the disease. This observation suggests that higher memory effects (corresponding to larger α values) lead to a swifter depletion of the susceptible human population, thereby intensifying disease transmission dynamics.

Moving to the second graph, we examine the infected human population during the same period. For lower α values, the infection peak experiences a delay, whereas higher α values cause the

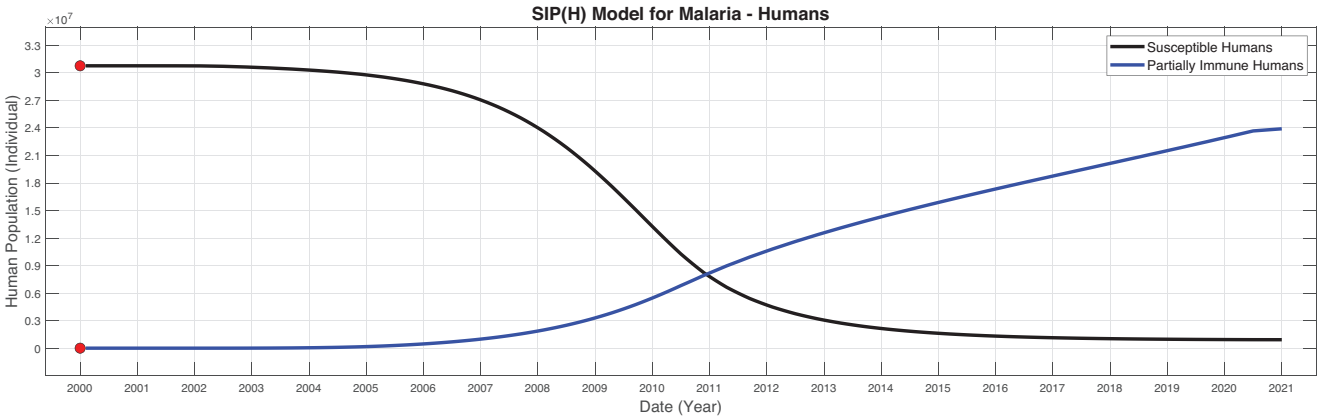

Figure 3. Numerical simulation results for the model for the human population.

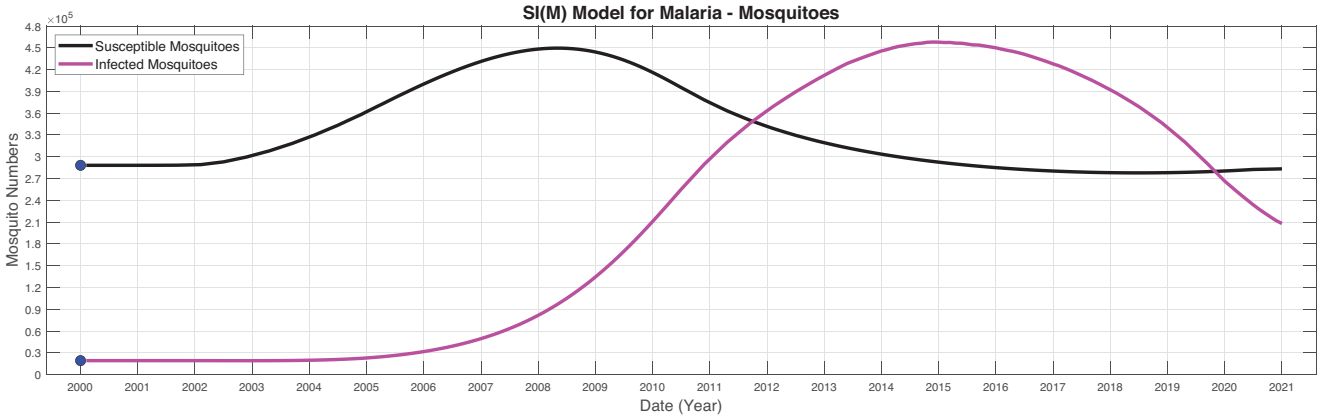

Figure 4. Numerical simulation results for the model for the mosquito population.

peak to manifest earlier and with greater intensity. This temporal shift in the infection peak for smaller α values provides a critical window for implementing intervention strategies that can mitigate the impact of the disease.

The third graph depicts the susceptible mosquito populations over time. Analogous to the human population, an increase in α results in a more rapid reduction in the number of susceptible mosquitoes. This behavior reflects the heightened transmission dynamics associated with larger α values.

These simulation results and accompanying graphs emphasize the pivotal role of the fractional-order parameter α in malaria transmission dynamics between humans and mosquitoes. Higher α values lead to rapid and intense disease spread, which affects human susceptibility and infection peaks. Conversely, smaller α values allow for delayed infection peaks, thereby creating an opportunity for early intervention. These insights underscore the significance of fractional models for understanding disease spread and optimizing public health strategies.

After the initial analysis, adjustments were made to the crucial parameter β, which represents the disease transmission rate among the infected individuals. Gradual and diverse modifications are applied to return to the initial baseline value, and the resulting impact on the populations of infected individuals is illustrated in **Figure 6** for the fractional cases, specifically with $\alpha = 0.85$ and $\alpha = 0.95$.

The graphical results reveal a pronounced reduction in the peaks of the infection curves within each population category as the contact rate β decreases. Notably, smaller values of the fractional parameter α correspond to a slower and more sustained disease spread, effectively capturing the memory effect inherent in the model. This biological interpretation underscores that increasing α accelerates disease transmission, whereas lower

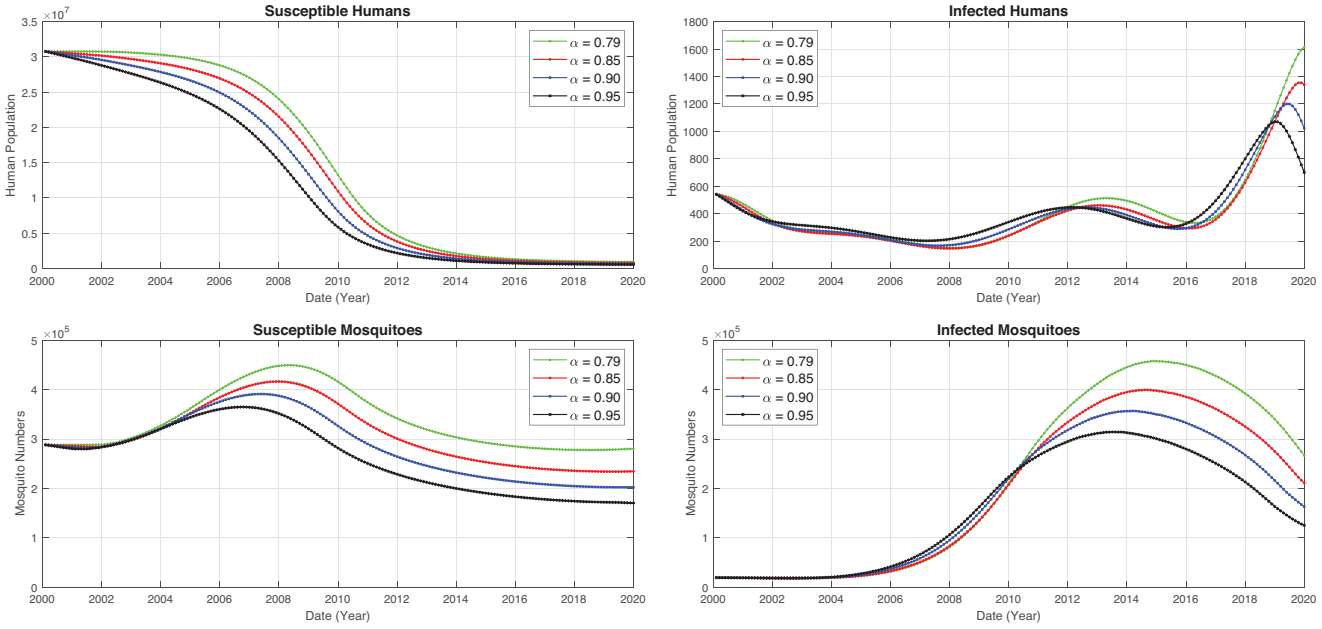

Figure 5. The dynamics of Caputo's fractional model for various values of α and using the estimation parameters in Table 2.

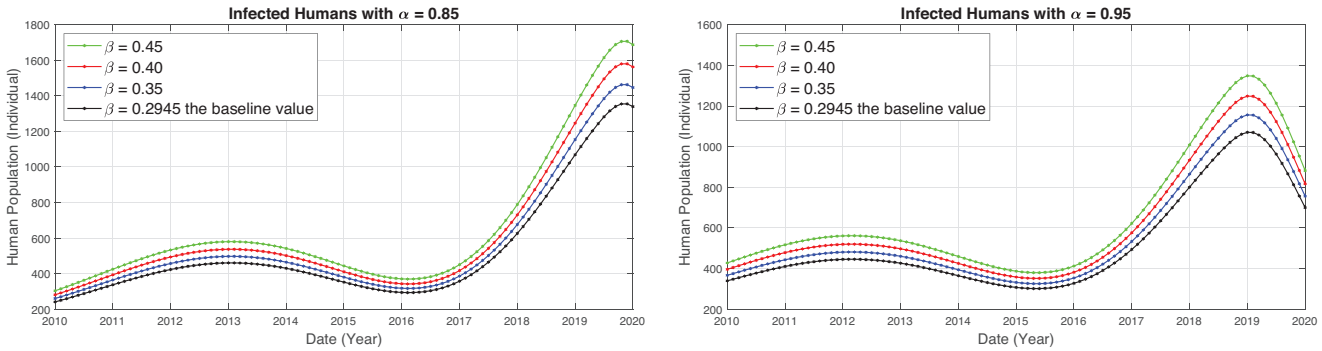

Figure 6. Impact of β on the infected population for different values of α with $\alpha = 0.85$, $\alpha = 0.95$ and using the estimation parameters in Table 2.

values delay the appearance of infection peaks, a behavior contingent upon the impact of preceding events.

Furthermore, our graphical analysis emphasizes the critical role of preventive measures. Neglecting interventions such as reducing human-mosquito contact, leads to a substantial increase in infections, facilitating a longer and swifter disease spread. Therefore, targeted efforts to minimize the contact between humans and mosquitoes should be central to intervention strategies. Implementing insecticides and medications to reduce mosquito populations significantly contributes to the maintenance of human population stability and curbing disease transmission.

5.3. Significance and Closing Remarks on Numerical Simulation

In Algeria, concerted efforts by authorities aim to raise public awareness about the critical importance of implementing safety measures to prevent malaria transmission. These preventive measures include targeted pesticide spraying in high-risk areas, distribution of treated mosquito bed nets for nocturnal protection, and provision of medications for treatment and prevention. Implementing these preventive strategies is pivotal for managing the spread of malaria as they effectively reduce the risk of infection and subsequent transmission.

In our mathematical model, these preventive measures directly impact the parameter β, which represents the rate of infection transmission from mosquitoes to humans. Our simulations explore how variations in this parameter influence disease progression and spread. Figures 5 and 6 illustrate how different values of the fractional-order parameter α affect the duration of the critical disease state, particularly the number of infected individuals. Specifically, $\alpha \in (0, 1)$ quantifies memory during epidemics. As α approaches zero, the system exhibits perfect memory, whereas approaching one signifies no memory. Notably, an increase in β leads to a rapid surge in the number of infected individuals, emphasizing that neglecting safety measures significantly accelerates disease spread.

A comparison of our results with those of recent studies employing traditional models reveals that the fractional-order model better captures the intricate dynamics of disease transmission, particularly in the context of malaria. Recent research utilizing fractional-order models has demonstrated their efficacy in providing more accurate epidemic predictions, especially when accounting for natural delays in transmission processes. Our model aligns with these findings, but introduces a novel dimension by explicitly considering the impact of memory on disease spread, an aspect overlooked in traditional models.

Table 2. Parameters and initial data of the SIP(H)–SI(M) model.

Parameter	Interpretation	Baseline Value	Reference
Λ	Recruitment rate of human	0.022818	Estimated [49]
S_H (0)	Initial number of S_H	30 773 545	Calculated
I_H (0)	Initial number of I_H	541	[48]
P_H (0)	Initial number of P_H	535	Assumed
S_M (0)	Initial number of S_M	288 232	Assumed
I_M (0)	Initial number of I_M	19 310	Assumed
β	Rate of transmission from I_M to S_H	0.294482673	Fitted
δ	Immunity loss rate of humans	0,0314446765	Fitted
κ	Immunity acquisition rate of humans	0,512191861	Fitted
λ	Recruitment rate of mosquito	0.104576629	Fitted
γ	Rate of transmission from I_H to S_M	0.126616512	Fitted
υ	Natural death rate of mosquitoes	0.456197917	Fitted
μ	Natural death rate of humans	0.0046818	Estimated [49]

6. Conclusion

This study conducted a comprehensive analysis of the SIP(H)–SI(M) model, affirming its efficacy in elucidating malaria transmission and spread dynamics. Our primary objective was to explore effective prevention, control strategies, and to draw insights from multiple studies that provide essential tools for predicting the impact of malaria and mitigating its effects.

From both epidemiological and mathematical perspectives, we delineated a suitable and feasible region for the model's solutions, and subsequently investigated their existence, uniqueness, and stability. Notably, our inquiry was extended to apply fractional operators within the SIP(H)–SI(M) model, specifically testing it in the context of Algeria. Parameters were meticulously estimated using real-world data, and numerical simulations illuminated the dynamic behavior of human and mosquito populations

over time. These simulations consistently revealed that higher infection transmission rates correlate with an increased number of infected individuals.

Remarkably, the disease-free equilibrium remained stable across all the numerical simulations when the basic reproduction number fell below unity. Our choice of Adams–Bashforth–Moulton numerical scheme offers distinct advantages over alternative methods: improved stability, faster convergence, and heightened accuracy in handling fractional epidemic models. These attributes make it particularly effective for studying intricate disease dynamics such as those observed in malaria, in which fractional calculus plays a pivotal role.

The performance demonstrated by this numerical approach significantly contributes to accurate predictions for effective control of malaria spread. Furthermore, our detailed analysis underscores the critical imperative of reducing the basic reproduction number below unity. Achieving this reduction requires targeted interventions, including treatment measures, and minimization of human-mosquito contact. Effective medications, insecticides, and treated bed nets emerge as pivotal tools for curbing mosquito populations and mitigating malaria transmission.

Acknowledgements

This work was supported by (DGRSTD)- Algeria.

Conflict of Interest

The authors declare no conflict of interest.

Data Availability Statement

The data that support the findings of this study are available in the supplementary material of this article.

Keywords

estimation parameters, existence and stability, malaria, mathematical modeling, numerical simulation

Received: June 30, 2024
Revised: September 24, 2024
Published online: November 6, 2024

[1] J. Li, *Math Biosci Eng* **2011**, *8*, 753.
[2] S. Olaniyi, OS. Obabiyi, *Int. J. Pure Appl. Math.* **2013**, *88*, 125.
[3] Osman MA-RE-N, Adu IK, C. A. Yang, *Asian Res J Math* **2017**, *7*, 1.
[4] J. Djordjevic, C. J. Silva, D. F. M. Torres, *Appl. Math. Lett.* **2018**, *84*, 168.
[5] F. Ndaïrou, I. Area, J. J. Nieto, C. J. Silva, D. F. M. Torres, *Math. Methods. Appl. Sci.* **2018**, *41*, 8929.
[6] A. Rachah, D. F. M. Torres, *Math. Comput. Sci.* **2016**, *10*, 331.
[7] A. Ullah, T. Abdeljawad, S. Ahmad, K. Shah, *J. Funct. Spaces* **2020**.
[8] P. A. Naik, M. Farman, A. Zehra, K. S. Nisar, E. Hincal, *Partial Differ. Equ. Appl. Math.* **2024**, *10*, 100663.
[9] P. A. Naik, A. Zehra, M. Farman, A. Shehzad, S. Shahzeen, Z. Huang, *Front. Phys.* **2023**, *11*, 1307307.
[10] S. Jamil, P. A. Naik, M. Farman, M. U. Sleem, A. H. Ganie, *J. Appl. Math. Comput.* **2024**, *70*, 3441.
[11] P. A. Naik, B. M. Yeolekar, S. Qureshi, M. Yeolekar, A. Madzvamuse, *Nonliner Dyn* **2024**, *112*, 11679.
[12] P. A. Naik, M. Yavuz, S. Qureshi, M. Naik, K. M. Owolabi, A. Soomro, A. H. Ganie, *Comput. Methods Programs Biomed.* **2024**, *254*, 108306.
[13] M. Farman, A. Shehzad, K. S. Nisar, E. Hincal, A. Akgul, *Comput. Biol. Med.* **2024**, *178*, 108756.
[14] K. S. Nisar, M. Farman, *Int. J. Model. Simul.* **2024**, 1.
[15] M. Farman, N. Gokbulut, U. Hurdoganoglu, E. Hincal, K. Suer, *Comput. Biol. Med.* **2024**, *173*, 108367.
[16] K. S. Nisar, M. Farman, A. Zehra, E. Hincal, *Int. J. Model. Simul.* **2024**, 1.
[17] K. S. Nisar, M. Farman, M. Abdel-Aty, C. Ravichandran, *Alex. Eng. J.* **2024**, *95*, 283.
[18] A. O. Atede, A. Omame, S. C. Inyama, *Bull. Biomath.* **2023**, *1*, 78.
[19] B. Basti, Y. Arioua, N. Benhamidouche, *Acta Math. Univ. Comenian.* **2020**, *89*, 243.
[20] B. Basti, B. Chennaf, M. A. Boubekeur, S. Bounouiga, *Adv. Theory Simul.* **2024**, *7*, 2301285.
[21] B. Basti, N. Hammami, I. Berrabah, F. Nouioua, R. Djemiat, N. Benhamidouche, *Symmetry* **2021**, *13*, 1431.
[22] M. D. Ortigueira, J. A. Tenreiro Machado, *J. Comput. Phys.* **2015**, *293*, 4.
[23] U. K. Nwajeri, A. Omame, C. P. Onyenegecha, *Results Phys.* **2021**, *28*, 104643.
[24] R. Toledo-Hernandez, V. Rico-Ramirez, G. A. Iglesias-Silva, U. M. Diwekar, *Chem. Eng. Sci.* **2014**, *117*, 217.
[25] B. Basti, N. Benhamidouche, *Surv. Math. Appl.* **2020**, *15*, 153.
[26] B. Basti, R. Djemiat, N. Benhamidouche, *Mem. Differ. Equ. Math. Phys.* **2023**, *89*, 1.
[27] R. Djemiat, B. Basti, N. Benhamidouche, *Adv. Theory Nonlinear Anal. Appl.* **2022**, *6*, 287.
[28] R. Djemiat, B. Basti, N. Benhamidouche, *Appl. Math. E-Notes* **2022**, *22*, 427.
[29] R. Djemiat, B. Basti, N. Benhamidouche, *An. Stiint. Univ. Al. I. Cuza Iasi. Mat.* **2023**, *69*, 143.
[30] R. L. Magin, *Fractional Calculus in Bioengineering*, Begell House, Danbury**2006**.
[31] F. Nouioua, B. Basti, *Ann. Univ. Paedag. Crac. Stud. Math.* **2021**, *20*, 43.
[32] S. Annas, M. I. Pratama, M. Rifandi, W. Sanusi, S. Side, Chaos, *Solit. Fract.* **2020**, *139*, 110072.
[33] A. A. Gebremeskel, H. E. Krogstad, *Am. J. Appl. Math.* **2015**, *3*, 36.
[34] C. Xu, W. Zhang, C. Aouiti, Z. Liu, L. Yao, *Math. Methods Appl. Sci.* **2023**, *46*, 9103.
[35] Y. Arioua, B. Basti, N. Benhamidouche, *Appl. Math. E-Notes* **2019**, *19*, 397.
[36] B. Basti, Y. Arioua, N. Benhamidouche, *J. Math. Appl.* **2019**, *42*, 35.
[37] B. Basti, N. Benhamidouche, *Appl. Math. E-Notes* **2020**, *20*, 367.
[38] B. Basti, Y. Arioua, *J. Math. Phys. Anal. Geom.* **2022**, *18*, 350.
[39] B. Lekdim, B. Basti, *Jordan J. Math. Stat.* **2024**, *17*, 199.
[40] A. Zeeshan, Z. Akbar, S. Kamal, *Hacettepe J. Math. Stat.* **2018**, *48*, 1092.
[41] J. P. LaSalle, *IRE Trans. Circuit Theory* **1960**, *7*, 520.
[42] C. Vargas-De-Leon, *Commun. Nonlinear Sci. Numer. Simul.* **2015**, *24*, 75.
[43] K. Diethelm, N. J. Ford, A. D. Freed, *Nonlinear Dyn.* **2002**, *29*, 3.

[44] K. Diethelm, N. J. Ford, A. D. Freed, *Numer. Algorithms* **2004**, *36*, 31.
[45] P. Roman, in *AIP Conference Proceedings, AIP Publishing LLC, Melville*, NY, USA, **2021**.
[46] R. Garrappa, *Int. J. Comput. Math.* **2010**, *87*, 2281.
[47] Algeria Population 1950-2024, https://www.macrotrends.net/countries/DZA/algeria/population (accessed: April 2024).
[48] Number of confirmed malaria cases, World Health Organization, https://www.who.int/data/gho/data/indicators/indicator-details/GHO/number-confirmed-malaria-cases (accessed: May 2023)
[49] Population growth in Algeria, https://www.donneesmondiales.com/afrique/algerie/croissance-population.php (accessed: Jan 2024).